Journal of Hydrology 626 (2023) 130335

Contents lists available at ScienceDirect

Journal of Hydrology

journal homepage: www.elsevier.com/locate/jhydrol

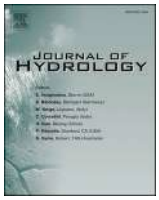

Research papers

Fish community traits near a large confluence: Implications for its nodal effects in the river ecosystem

Saiyu Yuan [a,b,b,*], Jiajian Qiu [a,*], Hongwu Tang [a,b], Lei Xu [a], Yang Xiao [a,b], Mengyang Liu [a], Colin Rennie [c], Carlo Gualtieri [d]

[a] The National Key Laboratory of Water Disaster Prevention, Hohai University, Nanjing, China
[b] Key Laboratory of Hydrologic-cycle and Hydrodynamic System of Ministry of Water Resources, Hohai University, Nanjing, China
[c] Department of Civil Engineering, University of Ottawa, Ottawa, Canada
[d] Department of Structures for Engineering and Architecture, University of Napoli Federico II, Napoli, Italy

ARTICLE INFO

This manuscript was handled by Sally Elizabeth Thompson, Editor-in-Chief, with the assistance of Anthony Parolari, Associate Editor

ABSTRACT

River confluences are nodes where the unique hydrological processes of two rivers meet, resulting in complex flow structure and water quality mixing processes. Thus, greater food availability and habitat complexity can occur at a confluence, making it a hotspot for fish productivity and diversity. Nonetheless, studies that relate fish community traits to specific habitat characteristics at large river confluences are limited. Two field surveys were conducted at the large confluence between the Yangtze River and the Poyang Lake outflow channel involving fish hydroacoustic detection, environmental DNA, and acoustic velocity profiling. The discharge ratios of this confluence in two surveys were similar, but the water quality conditions represented by turbidity differed greatly. The results demonstrated high spatial heterogeneity of fish density, size, and species near the confluence. In the Yangtze River with high flow velocity, the abundance of small-sized fish was substantially higher than that in Poyang Lake outflow channel with low velocity, while large-sized fish chose their habitats more freely between the two tributaries and post-confluence channel. The convergence of two tributaries created prominent spatial heterogeneity of habitat conditions in the post-confluence channel, thus highest fish abundance and species biodiversity occurred there. The species assemblage structure of the local fish community was greatly affected by the change of water quality, e.g., the intrusion of a turbid flow from Poyang Lake into the Yangtze River, and thus the exchange of fish communities between two tributaries was weakened. The present study highlights the ecological importance of river confluence in improving regional fish abundance and species diversity and provides the theoretical foundation for the conservation and management of the aquatic environment at the confluence and in the whole river ecosystem.

1. Introduction

Confluences act as critical nodes that connect different tributaries. The hydrological processes of the tributaries interact with each other and undergo drastic changes at their confluence (Hu et al., 2007; Li et al., 2022). The confluence affects the flow structure (Best, 1987; Yuan et al., 2016; Rhoads and Johnson, 2018), sediment transport (Riley and Rhoads, 2012; Yuan et al., 2018; Pickering and Ford, 2021), bed morphology (Best, 1988; Rhoads et al., 2009; Cheng et al., 2019), water quality mixing process (Campodonico et al., 2015; Tang et al., 2018; Yuan et al., 2019; Zhang et al., 2020) between each tributary, and inevitably leads to the formation of a unique and complex ecological pattern at the confluence (Rice et al., 2006; Hui et al., 2022). These tributaries may often have different habitat characteristics (e.g., temperature, suspended-sediment concentration, bed material, water chemistry, etc.) affecting the aquatic ecology near the confluence, and generally forming a large spectrum of habitat complexity in the post-confluence channel (Rice et al., 2006). Therefore, high fish abundances of diverse species occur at confluences (Fernandes et al., 2004; Röpke et al., 2016). Furthermore, confluences act as the nodal points for fish to migrate through the river network, including between rivers and lakes, which is necessary for the completion of their life cycle

* Corresponding authors at: The National Key Laboratory of Water Disaster Prevention, Hohai University, Nanjing, China.
E-mail addresses: yuansaiyu@hhu.edu.cn (S. Yuan), jiajianq@hhu.edu.cn (J. Qiu).

https://doi.org/10.1016/j.jhydrol.2023.130335
Received 1 February 2023; Received in revised form 21 June 2023; Accepted 1 October 2023
Available online 16 October 2023

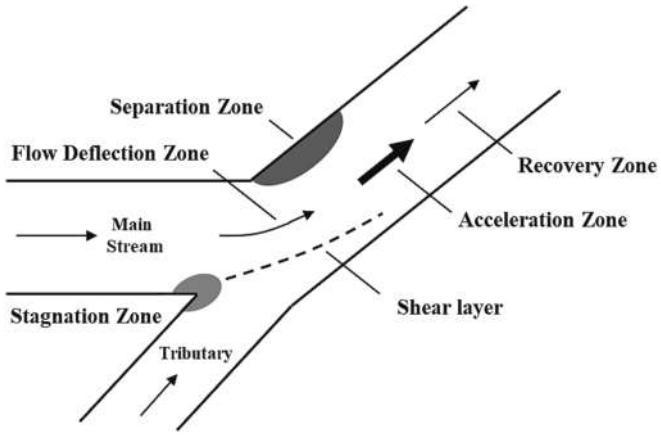

Fig. 1. Conceptual model of flow structures at channel confluences proposed by Best (1987).

(Northcote, 1996). For instance, confluence hydrodynamics play an active role in providing navigation cues for the migration of Chinook salmon to spawning habitats (Luis and Pasternack, 2023; Moses et al., 2019).

Fish communities are highly structured and the fish distribution depends upon a series of selective drivers, ranging from abiotic conditions to biotic interactions (Smith and Powell, 1971). The velocity distribution is an important driver for fish physiological processes, such as swimming, resting, spawning and predation. Asaeda et al. (2005) indicated that fish adopted different feeding behavior and habitat selection in varied flow velocities to keep the trade-off between feeding and swimming costs. Xu et al. (2017) pointed out that migratory fish need a threshold flow velocity to trigger their migration and identify the swimming direction. Additionally, in natural flows, the habitat preferences and biological activities of fish are also greatly influenced by complex flow structures and parameters (Crowder and Diplas, 2002), such as intensity, periodicity, vortex orientation, and vortex scale of the turbulence (Lacey et al., 2012), velocity gradient (Dabiri, 2017; Yuan et al., 2022a), shear stress (Silva et al., 2012), and other features. Scholars defined these spatiotemporal variations of flow patterns as hydraulic complexity, applied to investigate the influence on fish behaviors and identify the characteristics of fish habitats (Crowder and Diplas, 2000; Gualtieri et al., 2017, 2020).

In addition to flow structures, water environmental conditions also influence the fish habitat preference (Brown et al., 2004; Kramer, 1987). Water temperature is a critical determinant of fish metabolism and behavior, especially in influencing the spawning time and reproductive capacity of fish, which makes it an important driver for fish migration (Wenger et al., 2011). Dissolved oxygen affects fish habitat preferences and physiological processes, as both hypoxia and supersaturation can significantly reduce the survival rate of fish (Shen et al., 2019). Chlorophyll content can indicate the biomass of algae in water, which is an important food source for juvenile fish, and its fluctuation leads to long-term changes in fish recruitments (Vanni and Layne, 1997; Beaugrand et al., 2003). Turbidity largely determines the predator–prey interactions, as predator and prey species have differential orientating abilities in a turbid environment (Scarabotti et al., 2011; Sutherland and Meyer, 2007).

Flow structures at river confluences are highly complex and have three-dimensional features (Sukhodolov et al., 2017; Gualtieri et al., 2018, 2019). There are six different zones with distinct hydraulic characteristics (Best, 1987; Yuan et al., 2022b; Shen et al., 2022), namely stagnation zone, flow deflection zone, separation zone, acceleration zone, shear layer, and recovery zone (Fig. 1). In addition, complex coherent structures such as the Kelvin-Helmholtz vortices or wake vortices induced by velocity gradient across the shear layer (Constantinescu et al., 2011, 2012; Konsoer and Rhoads, 2014), and the helical cells formed by the deflection of flow from the tributaries that are dominated by streamwise-oriented vortices with strong upwelling or downwelling flows are also observed at confluences. These complex flow structures play an important role in the mixing process between tributaries with different water quality conditions (Best and Roy, 1991; Rhoads and Sukhodolov, 2008; Constantinescu et al., 2016; Shen et al., 2021; Duguay et al., 2022). Xu et al. (2022) observed a slow mixing process during high-flow conditions as dual counter-rotating secondary cells existed, with the downwelling flow acting as a barrier to prevent the exchange of two flows, while a single channel-scale secondary flow accelerated the mixing during low-flow conditions at the confluence between the Yangtze River and Poyang Lake (near 29.75°N, 116.22°E). The complex flow structures and distinct distribution pattern of water quality at confluences greatly influence the habitat selection of fish communities and the processes of fish migration through confluences.

Previous field surveys have investigated the distribution of fish communities and their habitat characteristics at river confluences. Braaten and Guy (1999) sampled fish from seven different confluences in the Missouri River (near 44.35°N, 100.37°W), and concluded that the choice of fish habitat strongly depended upon the spatiotemporal changes in physicochemical parameters such as discharge and water temperature. However, these surveys were conducted in small- and medium-scale confluences with width-to-depth ratios of less than 50, and the features observed in such confluences might not be representative of large-scale confluences. Large river confluences have a broader range of inflow conditions, such as discharge, water quality, sediment concentration, and a more prominent habitat heterogeneity for fish communities. Also, fixed-point fishing with nets, such as electric fishing and gillnet fishing, often fails to capture accurate relations between fish distribution and the habitat factors. Nets can only catch fish randomly in a large area and cannot demarcate how fish use the microhabitat within the area. Furthermore, while some field studies have associated spatial distributions and movement processes of fish to hydraulic characteristics of the river (e.g., Bergman et al., 2023), most studies relating swimming behavior of fish and their spatial distribution to habitat factors have been conducted through laboratory experiments and numerical simulations (Olivetti et al., 2021; Yuan et al., 2022a). Inevitably, these results present differences as compared to natural field situations.

In the present study, two field surveys using non-invasive fish detection methods, acoustic Doppler velocity profiling, and water quality measurements were carried out at the large confluence between the Yangtze River and the Poyang Lake outflow channel. The confluence between the Yangtze River and the Poyang Lake outflow channel is a key node for the interaction of fish communities in the river and lake. Migratory fishes represented by the four major Chinese carps (black carp, grass carp, silver carp, and bighead carp), the important commercial fish in China, migrate through the confluence every year to fulfill the specific habitat requirements at different stages of their life history, such as breeding, foraging, escaping from seasonally adverse weather conditions, and avoiding predators (Song et al., 2018).

The present study aims to determine (1) the distribution patterns of hydraulic and water quality parameters that influence fish communities; (2) the abundance distribution and species assemblage structure of fish communities; and (3) the driving effects of those hydraulic and water quality parameters on fish communities at a large river confluence.

It is hypothesized that the large river confluence is a hotspot for fish biodiversity, which can substantially increase the abundance and species diversity of fish community downstream, and the spatiotemporal heterogeneity of hydraulic and water quality parameters of the merging flows affects different aspects of the distribution of fish communities at the confluence. Understanding the driving effect of different hydraulic and water quality parameters on the fish community traits at the confluence will enrich the knowledge of the ecological process at river confluences and support protection and restoration of riverine ecosystems.

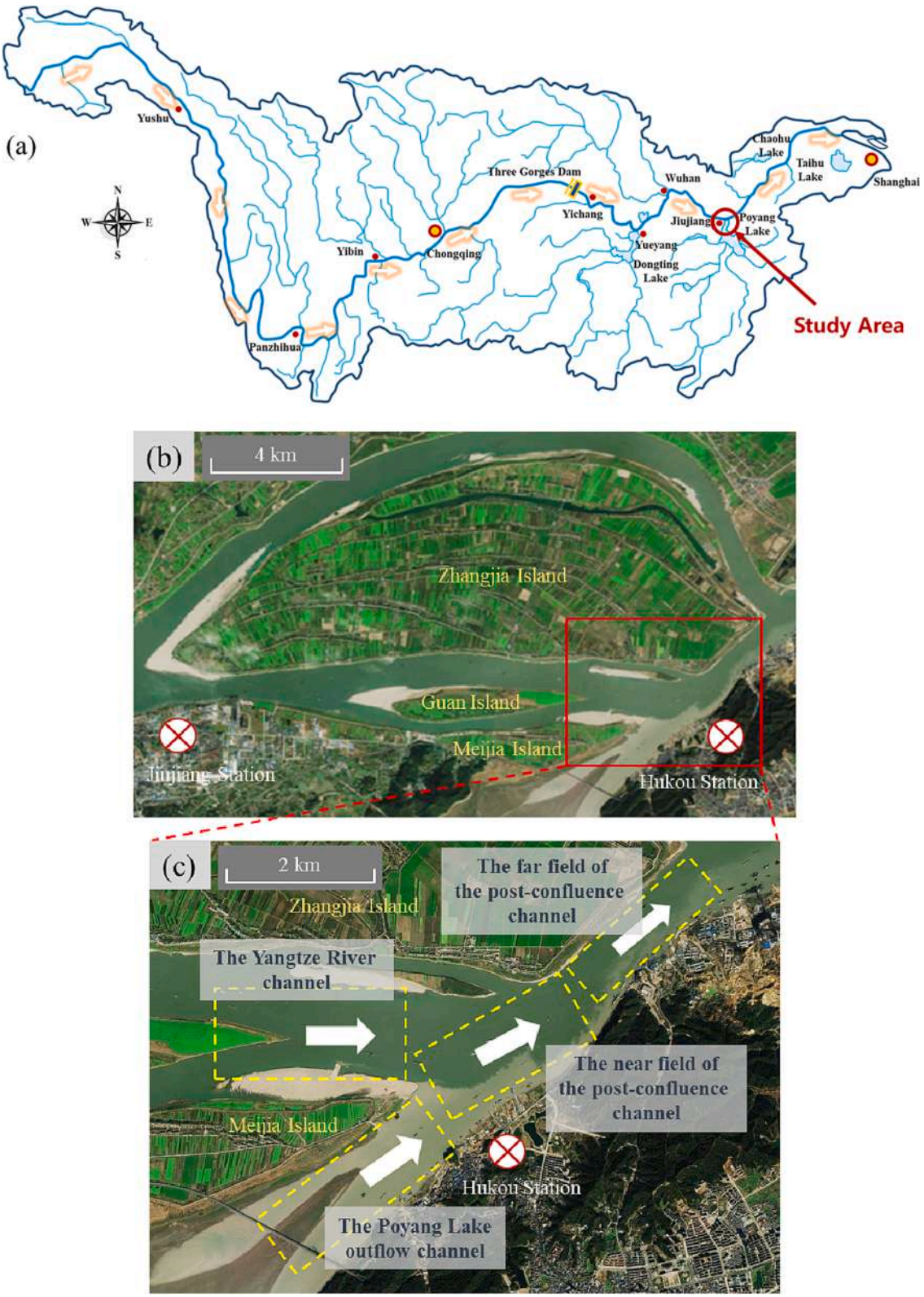

Fig. 2. (a) Map of the Yangtze River catchment showing the confluence between the Yangtze River and Poyang Lake is in the middle and lower reaches of the Yangtze River (near 29.75°N, 116.22°E), the glowing arrows indicate the flow direction of the Yangtze River. (b) Locations of hydrological stations and islands near the confluence. (c) General locations of each region at the confluence, and white arrows indicate the flow direction in each region. (d) The light blue dashed lines mark the survey trajectory for the fish hydroacoustic detection and water quality measurements. (e) Map of the measurement locations at the confluence. The yellow lines mark cross-sections for the measurement of the flow field, while the circular symbols indicate environmental DNA sampling sites. (For interpretation of the references to color in this figure legend, the reader is referred to the web version of this article.)

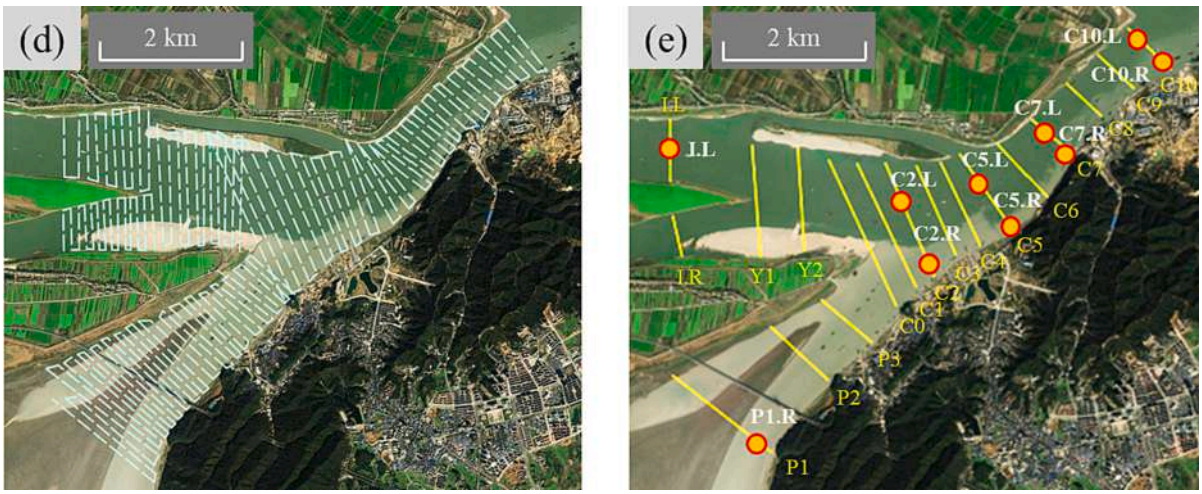

Fig. 2. (*continued*).

2. Methods

2.1. Study area

The Yangtze River has one of the largest drainage basins in the world, with relatively intact freshwater ecosystems and a quite abundant biodiversity. There are 463 species of indigenous fish in the Yangtze River catchment, among which 183 species are endemic, accounting for half of the total number of endemic fish in China (Lin et al., 2021). Poyang Lake Basin is located at the middle and lower reaches of the Yangtze River, with an area of 162,200 km^2 and accounting for 9 % of the Yangtze River catchment. As the largest river-connected lake of the Yangtze River, Poyang Lake plays an important role in supporting the biodiversity of the whole catchment and provides diverse habitats for numerous fish communities. Poyang Lake mainly recharges freshwater from the five upstream tributaries, and discharges via the confluence between the Yangtze River and the Poyang Lake outflow channel at Hukou (near 29.75°N, 116.24°E). The confluence is located at about 900 km downstream of the Three Gorges Dam and is 800 km upstream of the Yangtze River estuary (Fig. 2a). Near the Jiujiang Station, Zhangjia Island divides the Yangtze River into two branches. The one located on the south side of Zhangjia Island meets the Poyang Lake outflow, forming a confluence with a meeting angle of about 58°. It then rejoins with the other branch at around 5 km downstream of the confluence at an angle of nearly 90° (Fig. 2b).

This study focuses on the confluence between the Yangtze River and the Poyang Lake outflow channel. It covers an area of about 14 km^2, which includes part of the Yangtze River upstream of the confluence (hereafter referred to YR), the Poyang Lake outflow channel (PL), and the post-confluence channel (PC). The upstream part of the post-confluence channel exhibits special hydrodynamic features of confluences and is designated as the near field of the post-confluence channel (NPC). The downstream part is specified as the far field of the post-confluence channel (FPC). The specific boundaries of each region in the present survey are shown in Fig. 2c.

Two field surveys were carried out at the confluence in April (Survey 1) and October (Survey 2) 2021. These timings have special significance for the reproduction of local fish communities, including spawning, hatching, and growth of juvenile fish. In April, the discharge and water temperature gradually increase and the reproduction of local fish communities takes place. The reproduction period extends to October, when there is still a considerable number of newborn juvenile fish entering the Poyang Lake from the Yangtze River for rearing (Liu et al., 2019). The species assemblage structure of the fish community near the confluence does not change significantly unless the habitat environment is modified by external disturbance (Yang et al., 2022; Fang et al., 2023). This feature enabled us to analyze better the driving effects of changing habitat factors on the fish community. Moreover, the flow conditions of the river and its tributary were similar during the two surveys according to the records of Jiujiang and Hukou hydrology stations (Fig. 3). Therefore, it was possible to segregate the effects of water quality factors on the fish community, as the controlling hydraulic parameters were unchanged.

2.2. Hydraulic parameters measurements

An acoustic Doppler current profiler (aDcp), namely a Sontek River Surveyor M9 instrument, was used to collect cross-sectional measurements of three-dimensional velocity and bed profiles at key locations around the confluence. The transducer was anchored on the right side of the survey vessel, fixed at 0.5 m under the water surface and aimed vertically downward. A total of 18 cross-sections for the two tributaries and the post-confluence channel were selected (Fig. 2e). The field procedures for data acquisition and the data post-processing have been described in detail in Yuan et al. (2021).

A hydraulic complexity metric M_2 for quantifying and distinguishing flows with similar velocity values but different spatially varying flow patterns (Crowder and Diplas, 2000) was used to describe the hydraulic complexity of fish habitat at the confluence. The metric M_2 is proportional to the drag force on an organism moving from one location to another. It indicates the average rate of change in kinetic energy per unit mass and unit length between two points (Gualtieri et al., 2017, 2020), and is calculated by:

$$M_2 = 2v_{\mathrm{avg}}\frac{\left|\frac{(v_2-v_1)}{\Delta s}\right|}{v_{\mathrm{min}}^2} \tag{1}$$

where v_1 and v_2 are depth-averaged velocities measured in points 1 and 2, respectively, with a distance Δs along the direction of the predesigned cross-section, v_{avg} is the average value of v_1 and v_2, and v_{min} is the minimum value of v_1 and v_2. The median value of the Δs for calculating the metric M_2 was about 1.5 m, satisfying the general recommendations of Crowder and Diplas (2000) which consider the size of fish regarding the distance it may travel to obtain food, and similar value of the Δs have been used in another large confluence of Negro and Solimões rivers by Gualtieri et al. (2020). The metric M_2 was computed along each sampling cross-section, using depth-averaged velocity profile data acquired by aDcp, and its values were interpolated with the kriging procedure.

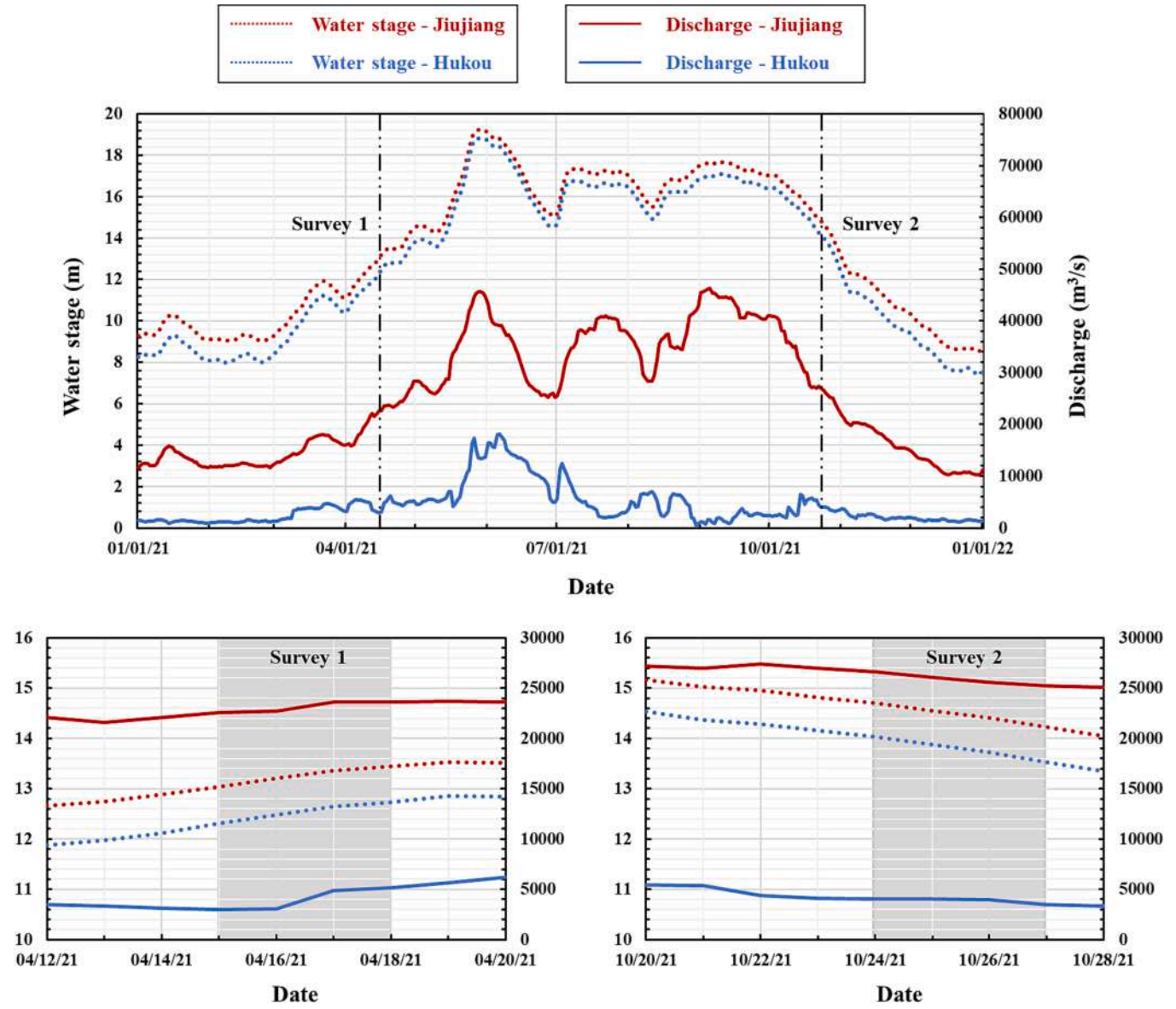

Fig. 3. Annual variation of water level and flow discharge at Jiujiang and Hukou stations in 2021, and timing of the two surveys. The water level is according to the frozen base level whose zero datum is 1.91 m higher than that of 1985 National Height Datum. The grey zone corresponds to the survey dates of the two surveys.

2.3. Water quality parameters measurements

Temperature, dissolved oxygen concentration, chlorophyll content and turbidity near the water surface were measured using a YSI EXO2 multi-parameter probe. The EXO2 probe was deployed at the left side of the survey vessel, and its sensors were fixed at 0.5 m below the water surface. The survey vessel traveled according to the trajectory shown in Fig. 2d. The field procedures for data acquisition and the data post-processing have been described in detail in Xu et al. (2022). In addition, the water quality data measured at PL, YR, NPC, and FPC were respectively averaged across the whole area to determine the original water quality conditions in the Yangtze River and Poyang Lake before the confluence and the mixing process of the two tributaries in the post-confluence channel.

Table 1
Parameter configuration in Visual Analyzer 4.1.

Parameters	Setting
Echo Threshold (dB)	−60
Correlation Factor	0.9
Min Plus Width Factor	0.75
Max Plus Width Factor	3
End Point Criteria (dB)	−12
Tracking Window (m)	0.2
Min Consecutive Echoes to Start Track	3
Min Additional Echoes to Accept Track	0
Max Ping Gap	2
Max Pings to Accept Track	50

2.4. Fish hydroacoustic detection

A BioSonics DT-X split-beam echosounder, with a 430 kHz transducer and 7° beam width, was employed for fish hydroacoustic detection, specifically, to detect the abundance and size distribution of fish. The echosounder transducer was anchored on the left side of the vessel together with the EXO2 probe, with the transducer fixed at 0.5 m under the water surface and aimed vertically downward. The measuring route was the same as that of the water quality measurements (Fig. 2d). The echosounder system was calibrated before the survey using the calibration ball. Acoustic data were acquired using BioSonics Visual

Table 2
Main hydraulic parameters at the confluence of the Yangtze River and the Poyang Lake outflow channel.

Region	Characteristic parameters	Survey 1 in April 2021	Survey 2 in October 2021
Poyang Lake outflow channel (P3 cross-section)	Wetted area A_{PL} (km^2)	2.24	3.94
	Mean depth H_{PL} (m)	9.72	8.11
	Maximum depth $Hmax_{PL}$ (m)	18.88	19.85
	Discharge Q_{PL} (m^3/s)	3137	4393
	U_{PL} (m/s)	0.51	0.41
Yangtze River channel (Y2 cross-section)	Wetted area A_{YR} (km^2)	3.70	4.65
	Mean depth H_{YR} (m)	8.96	9.07
	Maximum depth $Hmax_{YR}$ (m)	17.36	18.35
	Discharge Q_{YR} (m^3/s)	10,878	14,176
	U_{YR} (m/s)	0.95	0.98
Post-confluence channel (C1 cross-section)	Channel Width b (m)	2130	2350
	Discharge ratio $_{Qr}$	0.29	0.31
	Velocity ratio U_r	0.54	0.42
	Momentum ratio M_r	0.16	0.13

Note: U = average value of the cross-sectional velocity measured with aDcp; $Q_r = Q_{PL} / Q_{YR}$, $U_r = U_{PL} / U_{YR}$, $M_r = \rho_{PL} Q_{PL} U_{PL} / (\rho_{YR} Q_{YR} U_{YR})$, assuming $\rho_{PL} \approx \rho_{YR}$, where ρ indicates fluid density.

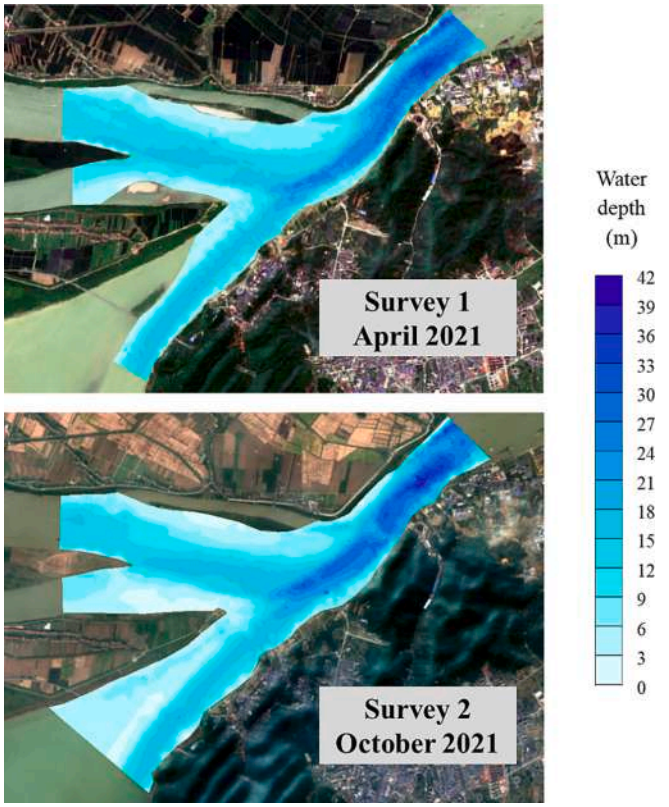

Fig. 4. Bathymetry of the confluence of the Yangtze River and the Poyang Lake outflow channel during Surveys 1 and 2.

Acquisition software, and the setting of acquisition parameters (e.g., pulse duration of 0.1 ms and pulse rate of 4 pps) for the measurement was determined according to the site-specific environmental conditions such as temperature and salinity.

The acoustic data were processed with BioSonics Visual Analyzer software 4.1. To avoid the interference of the bottom and bubbles near the water surface, only data pertaining to depths ranging from 1 m below the water surface to 0.5 m above the bottom were analyzed. The echo signals were compensated by time varied gain (TVG) depending on the range (R, m) between the target to the transducer. A $40\log_{10}R$ TVG was applied to the measurements of the Target Strength (TS, the strength of a returning echo from an individual fish, served as a fish length proxy (Egerton et al., 2021)), whereas a $20\log_{10}R$ TVG was used for the measurements of volume backscattering strength (Sv, served as a relative proxy for fish biomass (Boswell et al., 2010)). The acoustic data were divided into several units at 10 s intervals. The fish density of each unit was calculated via echo integration, defined as the backscattering coefficient per volume of water (sv, the linear equivalent of Sv) divided by the mean cross-sectional backscattering coefficient (σ_{bs}, the linear equivalent of TS from individual fish).

It should be noted that the hydroacoustic detection constantly undergoes interference from noise, especially in flows with high velocity and high suspended sediment concentration (Brehmer et al., 2006). Appropriate thresholds and manual correction were adopted to enumerate fish targets correctly. For instance, a threshold from −60 to −25 dB for TS was set to remove the noise from bubbles, plankton, and

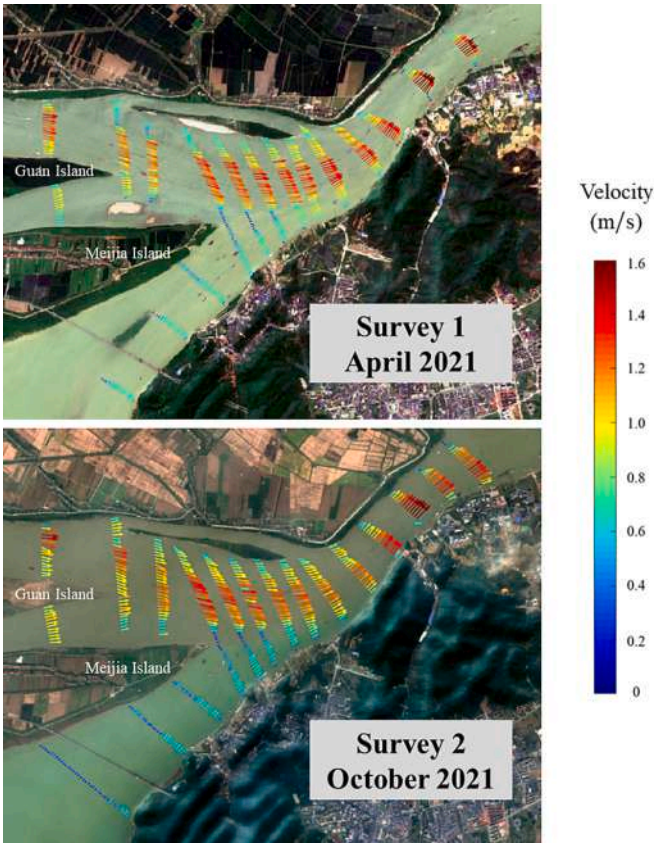

Fig. 5. Map of the depth-averaged velocities about the confluence of the Yangtze River and the Poyang Lake outflow channel during Surveys 1 and 2.

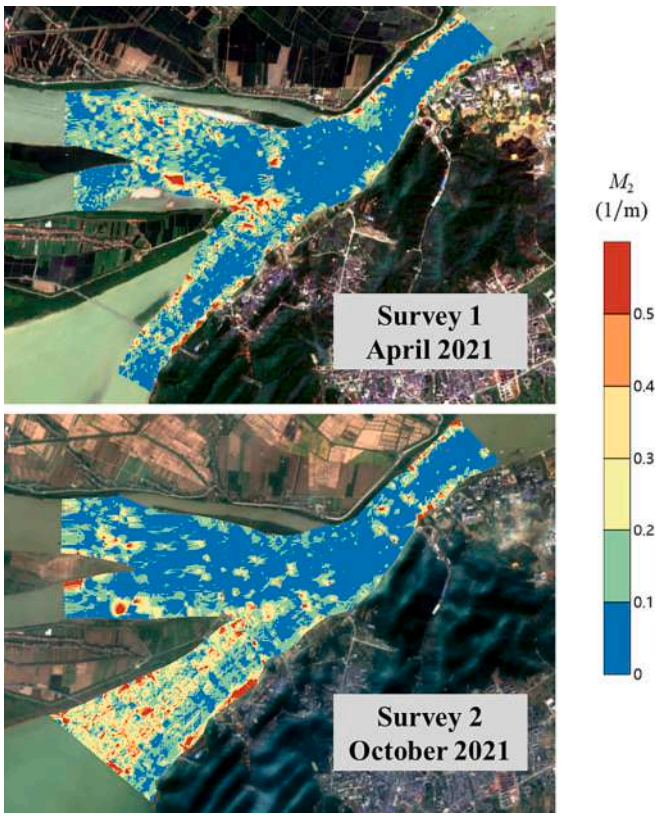

Fig. 6. Map of the metric M_2 about the confluence of the Yangtze River and the Poyang Lake outflow channel during Surveys 1 and 2.

other targets smaller than 2 cm or larger than 120 cm. The values of the remaining fish tracking parameters are listed in Table 1. The calculated fish density data were subsequently exported and interpolated by the ordinary kriging method.

Fish sizes were obtained from TS based on an empirical equation of Love (1971):

$$\mathrm{TS} = 19.11\log_{10}L - 0.9\log_{10}F - 62 \quad (2)$$

where L means the length of fish and F means the frequency of the transducer ($F = 430$ Hz in this work). To compare the differences in fish sizes among different survey areas, detected fish were divided into small-, mid-, and large-sized categories according to their length, using the classification method of Bean et al. (1996). Length of each size category ranges from 2 cm $< L <$ 20 cm (−60 to −40 dB), 20 cm $< L <$ 60 cm (−40 to −30 dB), and $L >$ 60 cm (greater than −30 dB).

2.5. Environmental DNA sampling and analysis

Environmental DNA offers a powerful tool capable of sensitively detecting fish species and approximatively reflecting the relative abundance of different species (Hänfling et al., 2016). In the present study, environmental DNA was sampled immediately following the hydroacoustic detection at 10 predesigned sites shown in Fig. 2d. The sampling sites were set at suitable distance from each other to ensure adequate coverage of the study area and to avoid interference between samples. Two sampling sites were set on cross-sections I-L and P1, respectively, to ascertain the fish species in the Yangtze River and Poyang Lake. Two sampling sites on cross-sections C2, C5, C7, and C10 in the post-confluence channel were selected to investigate the difference in fish species assemblage structure across the two sides of the channel. Sampling sites on the same side of the channel were at least 1 km apart, to minimize the accumulation of the upstream eDNA particles to downstream, as Jo and Yamanaka (2022) simulated the transport distance of eDNA particles downstream in lotic systems and found that nearly 95 % of eDNA particles were deposited when transported over 1 km. Three surface-water samples of 1 L volume were collected using sterile bottles at each site, and a bottle of ultrapure water was placed at the same time among the sampling bottles as a reference to check contamination during the sampling processes. Samples were vacuum filtered through a 0.45 μm filter membrane within 24 h. After filtration, the used membranes were folded up, placed in centrifuge tubes, and stored at −20 ℃ for extraction on the following day.

DNA from each filter membrane was extracted, amplified, and sequenced for subsequent bioinformatic analysis. The detailed descriptions for extraction, amplification, and sequencing protocol can be found in previous publications (e.g., Xie et al., 2021). To generate a high-confidence dataset, low-confidence and spurious annotations were removed as false positives according to Port et al. (2016). Finally, the relative abundance of each identified fish species is represented by its sequencing reads.

Based on the environmental DNA sequencing result, the dominant species are determined according to McNaughton index Y_i:

$$Y_i = p_i f_i \quad (3)$$

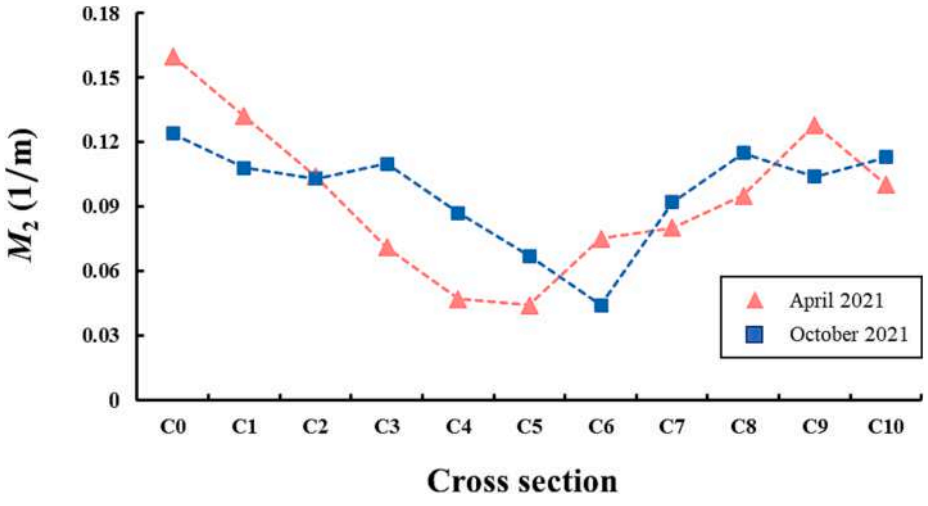

Fig. 7. Longitudinal distribution of the cross-sectional mean M_2 based on the depth-averaged velocity along the post-confluence channel between the Yangtze River and the Poyang Lake outflow channel during Surveys 1 and 2.

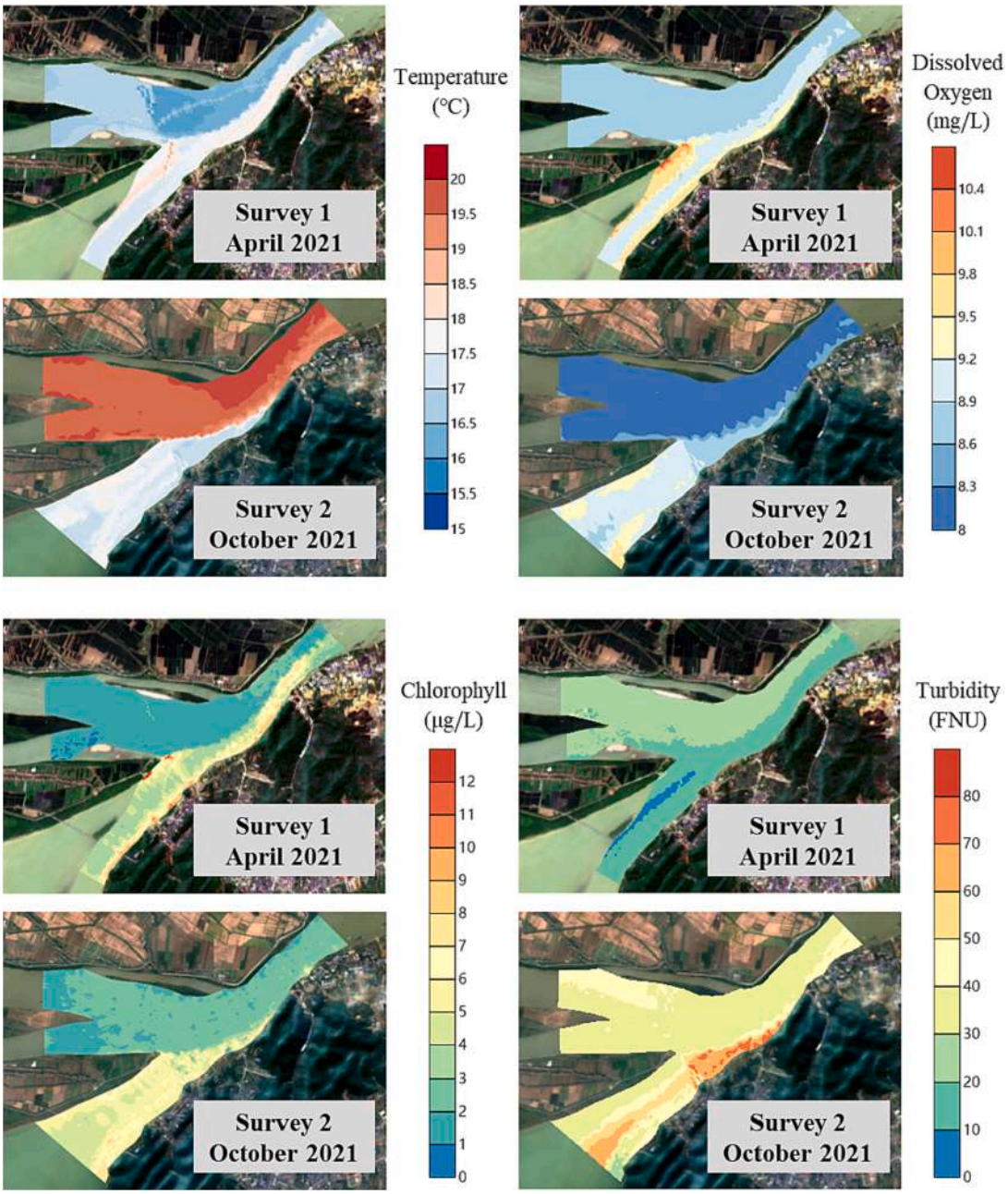

Fig. 8. Map of the temperature, dissolved oxygen concentration, chlorophyll content, and turbidity about the confluence of the Yangtze River and the Poyang Lake outflow channel during Surveys 1 and 2.

where p_i is the proportion of the i^{th} species reads to the total reads, f_i is the frequency of the i^{th} species detected among all sampling sites. A species is regarded as dominant when its Y_i is higher than 0.05 in this work.

Biodiversity indexes for fish, including Shannon-Weiner index (H_j'), Simpson index (D_j), and Pielou index (J_j') were calculated using Eqs (4)–(6) with species composition data to describe fish diversity in each sampling site:

$$H_j^{'} = -\sum_{i=1}^{S_j} p_{ij} \ln p_{ij} \tag{4}$$

$$D_j = 1 - \sum_{i=1}^{S_j} p_{ij}^2 \tag{5}$$

$$J_j^{'} = \frac{H_j^{'}}{\ln S_j} \tag{6}$$

where S_j is the species number identified in the j^{th} sampling site, p_{ij} is the proportion of the i^{th} species reads to the total reads in the j^{th} sampling site.

2.6. Ordination and statistical analysis

Based on hierarchical cluster analysis of $\log_{10}$-transformed relative abundance data, fish species were grouped with similar distribution patterns among sampling sites in the two surveys. The cluster analysis was performed by UPGMA (unweighted pair-group method with arithmetic means) clustering method with Euclidean distance. Likewise, the grouping of sampling sites was determined by the similarity in the

relative abundance of species between sites. The similarities were assessed by the Pearson correlation coefficient, and UPGMA clustering method was based on Euclidean distance.

In order to distinguish the driving effects of habitat factors, such as water depth (*H*), flow velocity (*v*), hydraulic complexity metric M_2, temperature (*T*), dissolved oxygen concentration (*DO*), chlorophyll content (*Chl*), and turbidity (*Turb*), on abundance distribution and species assemblage structure of fish communities, a redundancy analysis (RDA; R package "vegan", function "ca") was applied. This analysis relates fish community data with habitat characteristics of the sampling sites of the two surveys. The fish density acquired by hydroacoustic detection, the number of species identified by environmental DNA, three biodiversity indexes (Shannon-Weiner index, Simpson index, and Pielou index), and the relative abundance of four dominant fish species (*Zacco platypus*, *Hypophthalmichthys molitrix*, *Pseudorasbora parva*, and *Coilia nasus*, species with Yi higher than 0.05 during the two surveys) were considered as factors indicative of the fish community traits and thus were analyzed.

3. Results and discussion

3.1. Distribution patterns of hydraulic parameters

The main hydraulic parameters of the confluence region were calculated from aDcp measurements collected during the two surveys, and are listed in Table 2. The water depths of PL and YR in Survey 2 (October 2021) were both deeper than those in Survey 1 (April 2021), and a larger wetted area in Survey 2 was observed due to inundation of the floodplain along the channels (Fig. 4). With an increase of the flow area, the average velocity decreased in PL, while that of YR remained basically unchanged, so that a lower velocity ratio U_r resulted in Survey 2 than in Survey 1. Nearly identical discharge ratios Q_r (~0.30) were observed during Surveys 1 and 2. The discharge and flow velocity in YR were both much higher than that in PL, leading to low momentum flux ratios M_r in both surveys (0.16 and 0.13, respectively). The thalwegs in the YR (maximum water depth: 17.4 m; minimum depth: 11.7 m) and PL (maximum depth: 39.8 m; minimum depth: 13.6 m) had no obvious deflection along the channel direction, while the thalweg in PC (maximum depth: 21.5 m; minimum depth: 14.4 m) was inclined towards the right bank due to the bend flow as well as the low Q_r and M_r. The water depth of the thalweg gradually increased, reaching its maximum value at about the end of the post-confluence channel.

Flow from the upstream of YR bifurcates at the Guan Island into two branches, the left branch has larger discharge and flow velocity; on the other side, PL had a relatively uniform and low depth-averaged velocity (Fig. 5). In general, the velocity magnitude of Survey 2 was lower than that of Survey 1, and the lowest velocity was at the inundated floodplain on the left side of PC in Survey 2. PC received flows from YR and PL, and a stagnation zone developed with very low velocity at the apex of the confluence near Meijia Island. A shear layer with velocity contrast between the two flows was observed. Due to the low M_r, the shear layer was forced to bend towards the right side of the channel. As the Poyang Lake outflow realigned with the Yangtze River flow, the velocity contrast gradually decreased, and the shear layer finally disappeared near the end of the NPC. As the width of the PC decreased and simultaneously the Poyang Lake outflow entered the confluence, the core velocity of the converging flow gradually increased. It reached the peak velocity in the FPC.

In both surveys, large values of metric M_2 were observed where the kinetic energy was relatively low, such as in the stagnation zone near the apex of the confluence, as well as along the bank in PL and FPC (Fig. 6). An extra region with large M_2 values was observed in Survey 2, on the submerged floodplain of PL due to the extremely low velocity there. The lowest M_2 values were found in the central part of PC, downstream of the stagnation zone, which is characterized by high flow velocity and significant flow deflection. The value of M_2 peaked immediately downstream of the confluence apex and then decayed gradually with the downstream distance until around the end of the NPC (Fig. 7). Following the fall, the value of M_2 gradually increased along the FPC.

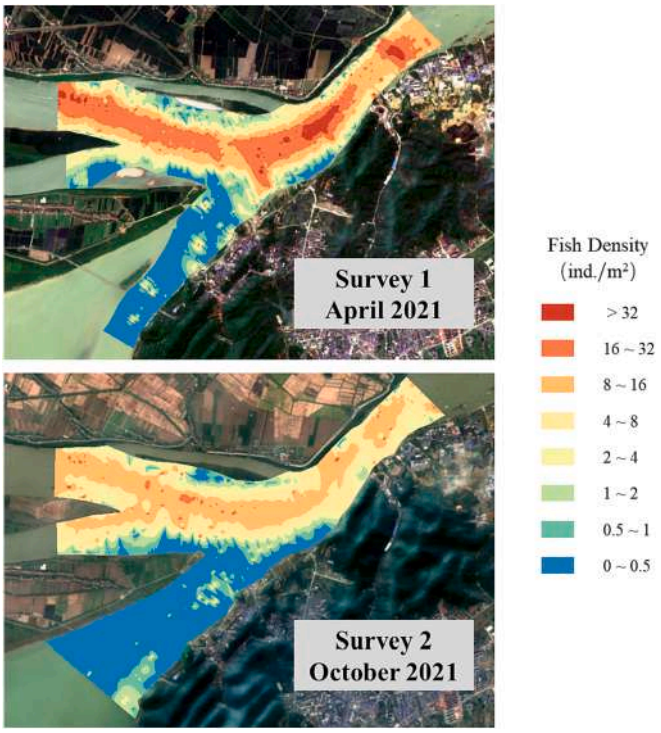

Fig. 9. Map of fish density (ind./m^2) about the confluence of the Yangtze River and the Poyang Lake outflow channel during Surveys 1 and 2.

Table 3
Average values of water quality parameters across the whole area of different regions near the confluence (PL, YR, NPC, and FPC) of the Yangtze River and the Poyang Lake outflow channel. Temperature (*T*), dissolved oxygen concentration (*DO*), chlorophyll content (*Chl*), turbidity (*Turb*).

		T (℃)	*DO* (mg/L)	*Chl* (μg/L)	*Turb* (FNU)
Survey 1 in April 2021	**PL**	17.38 ± 0.30	9.40 ± 0.34	5.33 ± 2.26	13.00 ± 2.94
	YR	16.73 ± 0.30	8.73 ± 0.13	1.48 ± 0.80	21.86 ± 3.72
	NPC	16.49 ± 0.70	8.96 ± 0.25	2.72 ± 2.04	19.32 ± 4.32
	FPC	16.92 ± 0.62	8.88 ± 0.18	3.46 ± 2.23	18.56 ± 4.10
Survey 2 in October 2021	**PL**	17.26 ± 0.30	9.11 ± 0.18	5.40 ± 0.92	45.23 ± 11.53
	YR	19.58 ± 0.03	8.24 ± 0.01	2.05 ± 0.29	40.51 ± 2.50
	NPC	18.97 ± 1.08	8.31 ± 0.22	2.99 ± 1.47	43.52 ± 12.52
	FPC	19.49 ± 0.25	8.23 ± 0.05	2.38 ± 0.49	38.47 ± 2.43

3.2. Distribution patterns of water quality parameters

Flows with distinctly different water quality conditions from the Yangtze River and Poyang Lake converged and mixed in PC (Fig. 8). In this process, a mixing interface between the two flows exists and a wider range of environmental conditions persists. During the period of Survey 1, a clear mixing interface was observed near the water surface, which persisted for a long distance. It extends until the end of PC, indicating a slow mixing process between the two incoming flows. Comparatively, in Survey 2 the mixing interface disappeared near cross-section C6, suggesting a faster mixing rate than in Survey 1. The larger lateral expansion of the Yangtze River flow into the Poyang Lake side in Survey 2 resulted from the larger momentum difference in Survey 2 ($M_r = 0.13$) compared with Survey 1 ($M_r = 0.16$). This explains why a more rapid mixing process and shorter mixing interface occurred in Survey 2.

The measured water quality parameters at different regions of the confluence were respectively averaged across the whole area, and the average values are listed in Table 3. In PL, the average temperature had little change between Surveys 1 and 2, both of which were about 17.30 ℃. In YR, the average temperature increased from 16.73 ℃ in Survey 1 to 19.58 ℃ in Survey 2, with an obvious rise of nearly 3 ℃. The temperatures in the NPC were between those in PL and YR in both Surveys 1 and 2, due to the mixing of the flow from PL and YR. With the proceeding of the mixing process, the temperatures in FPC gradually returned close to the original temperature in YR, since the flow from YR constituted a large proportion of the mixing flow. The other three water quality parameters also had a distribution pattern similar to that of the temperature, as PL and YR respectively kept the highest or lowest values. In the post-confluence channel, FPC had a value closer to that in YR compared to NPC. Furthermore, it is worth noting that a much larger turbidity near the water surface was observed in Survey 2 in all regions, nearly twice the value in Survey 1. The rise of turbidity in PL was especially high between the two surveys, where the turbidity in Survey 2 was nearly four times that in Survey 1. In contrast, dissolved oxygen concentration and chlorophyll content of each region near the confluence had similar values in Surveys 1 and 2.

3.3. Abundance distribution and species assemblage structure of fish communities

Fish density detected by hydroacoustic method in YR and PC were higher than that of PL in both Surveys 1 and Survey 2 (Fig. 9). In YR and NPC, most of the fish echoes were observed in the deep zone (with a water depth deeper than 10 m) in the central part of the channel, while only a low quantity of fish echoes was detected in the banks zone (with a water depth lower than 10 m). Although, it cannot be ruled out that the fish abundance in the bank zone is underestimated due to the increased escape of fish caused by the survey vessel in shallow waters. FPC had the highest fish density, with the most fish echoes still obtained in the deep zone, but also with increased observations in the banks zone because the channel was narrow. In PL, a lower number of fish echoes compared with the other regions was scattered in the banks zone and deep zone.

In both YR and PC, small-sized fish ($2\ \text{cm} < L < 20\ \text{cm}$) were dominant, accounting for more than 98 % of the total population, whereas mid-sized fish ($20\ \text{cm} < L < 60\ \text{cm}$) and large-sized fish ($L > 60$ cm) were relatively rare (Fig. 10). However, in PL the composition of the fish community, based on fish length, changed greatly from Survey 1 to Survey 2. The population of fish having a length of 2–3 cm increased dramatically, and its proportion to the total fish population surged from 23.01 % in April to 69.59 % in October. Percentage-wise the population

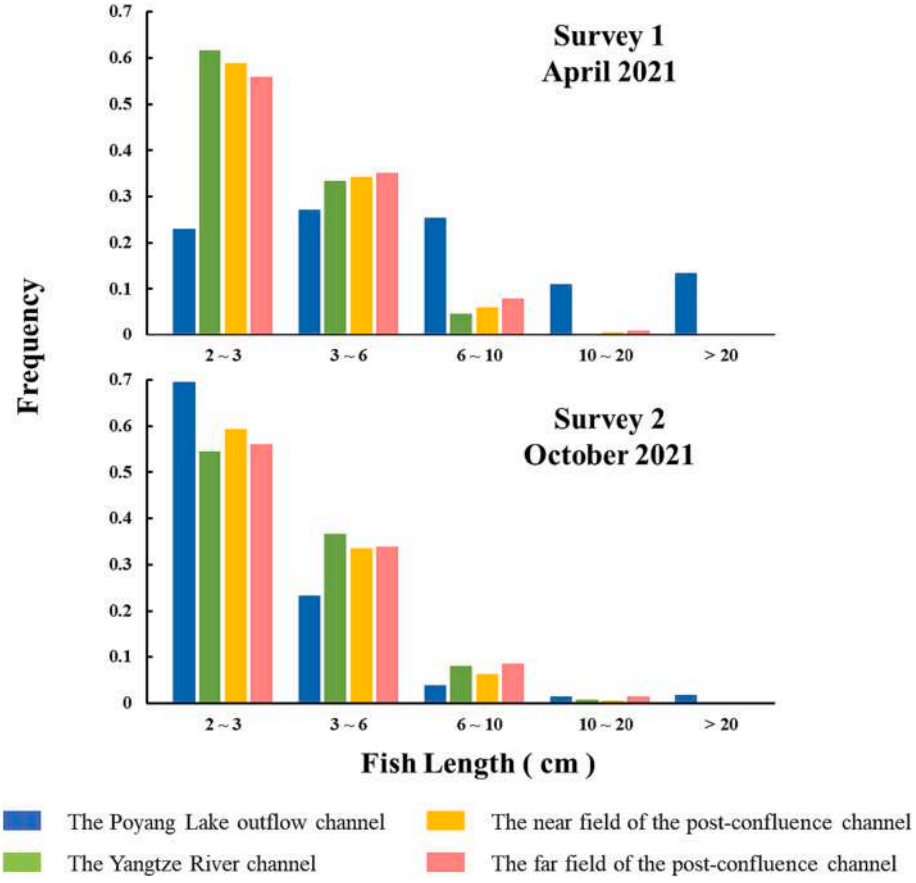

Fig. 10. Frequency distributions for the fish length in different regions of the confluence of the Yangtze River and the Poyang Lake outflow channel during Surveys 1 and 2.

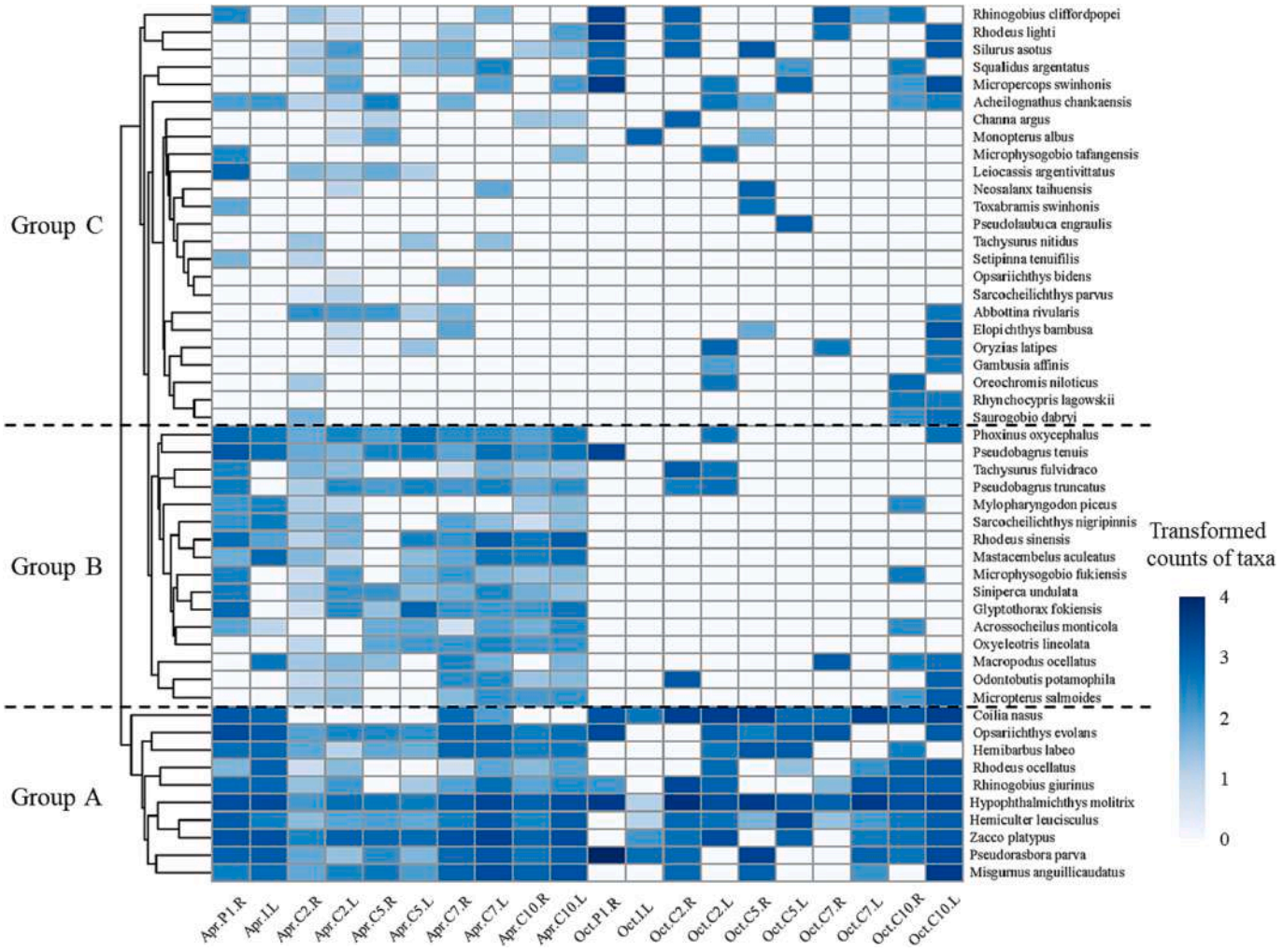

Fig. 11. Heatmap for $\log_{10}$-transformed counts of taxa identified with environmental DNA at each sampling site. The dendrogram shows the relationship of species based on UPGMA clustering method.

of fish larger than 6 cm in length reduced slightly, due to an increase in the total population. The changes in the proportion accounted by different fish lengths in the PL may be largely attributed to the influx of juvenile fish, following the spawning period, and the availability of additional habitat for small-sized fish provided by the inundated floodplain.

For the study on environmental DNA, a total of 50 fish species were identified in the two surveys, representing a diversity of 6 orders and 19 families (Fig. 11). The detected fish community was in general dominated by small-sized fish, and almost all the species observed in the present survey have previously been recorded in the middle and lower reaches of the Yangtze River (e.g., Liu et al., 2005; Fan et al., 2012). Many species, 47 of them, were detected in Survey 1, while 39 species were detected in Survey 2. Together, 36 of the same fish species were detected in both surveys, indicating that only a fraction of fish species observed in Survey 1 disappeared in Survey 2. Therefore, one can presume that there was no fundamental change in the assemblage structure of local fish communities. With regards to species diversity at different sampling sites, in Survey 1 a maximum value of 38 species were recorded in the initial part of PC (cross-section C2), whereas the highest number of fish species observed in Survey 2 was 23 at the downstream end of the study site (cross-section C10). In addition, the lowest fish diversity for both Surveys 1 and 2 was detected at the sampling site in YR, with 19 and 6 fish species, respectively. It is worth noting that, it was still difficult to determine whether the eDNA detected at each sampling site is fully representative of the fish community near the sampling site, although we tried to minimize the impact of upstream DNA on downstream species diversity.

According to the results of cluster analysis, the identified species were divided into three groups (as Group A, B, and C) based on their distribution patterns. The fish species in Group A were widely distributed in the study area and were relatively abundant at almost all sampling sites of both surveys, represented by silver carp (*H. molitrix*), *P. parva*, and *C. nasus*. Group B was comprised of species which were documented in Survey 1 but were rare in Survey 2, mainly including small-sized perciformes and siluriformes fish. Finally, the fish species distributed patchily throughout the confluence in both of the two surveys formed Group C, which was mainly composed of sedentary fish, including small fish such as bitterling (*Rhodeus lighti*) and goby (*Rhinogobius cliffordpopei*), as well as large fish such as catfish (*Silurus asotus*) and eel (*Monopterus albus*).

Higher number of species, Shannon-Weiner index, and Simpson index were observed in Survey 1 compared to Survey 2 (Fig. 12); it can be concluded that the confluence has higher fish species diversity in Spring rather than Autumn. However, there was no clear trend in the change of Pielou index between Surveys 1 and 2, indicating the uniformity of fish communities at the confluence had little relationship with seasonal changes. Furthermore, the number of species, Shannon-Weiner index, and Simpson index in YR were lower than those in PL and PC. It is possible that the connectivity due to the confluence helps the fish

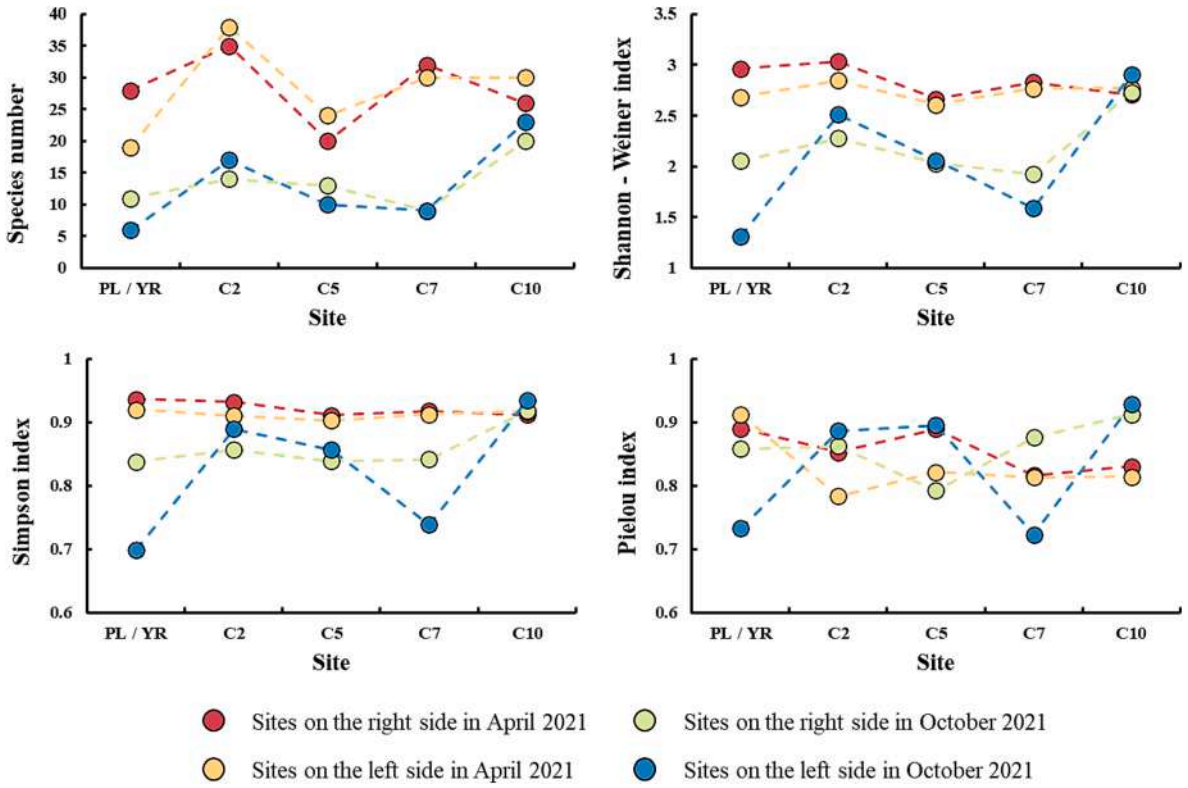

Fig. 12. Distribution of number of species and biodiversity indexes for fish among different sampling sites.

originating from Poyang Lake to enter the Yangtze River and enhances fish species diversity downstream of YR.

Based on the composition of the fish community at each sampling site, it was divided into two clusters through cluster analysis (Fig. 13). In Survey 1, a high similarity was observed among almost all sampling sites, indicating high connectivity and sufficient environmental capacity in April. However, the similarity in Survey 2 was relatively low, particularly the sampling site in YR had the lowest similarity with other sites. Although the connectivity of fish communities across the confluence seemed to be weakened in October, the inflow of Poyang Lake compensates the fish species assemblage structure in the Yangtze River. Furthermore, fish from the tributary preferred to migrate downstream rather than upstream when they entered the mainstream.

Spatial heterogeneities of fish community traits were expected at the confluence in both the surveys. In YR, quite high fish density was observed, while the species diversity was relatively low. On the contrary, the fish density in PL was much lower than other regions, but the fish diversity was considerable. Acting as a critical region connecting the Yangtze River and Poyang Lake, PC had the highest fish density and species diversity, and the exchange of different fish communities between the river and lake through the confluence might explain the extremely high fish productivity. Meanwhile, the two streams with different hydrodynamic and water quality conditions merged in the post-confluence channel, forming more prominent spatial heterogeneous habitat for fish. This is possibly another important reason for greater fish abundance and species diversity than those observed upstream.

3.4. Driving effects of habitat factors on fish communities

The redundancy analysis (RDA) for all sampling sites, constrained to hydraulic parameters (*H*, *v*, and M_2) and water quality parameters (*T*, *DO*, *Chl*, and *Turb*) is shown in Fig. 14. There is positive correlation between *T* and *Turb*, and the distribution patterns of these two factors are well represented by the axes-one of RDA. As Survey 2 had higher values of *T* and *Turb* compared to Survey 1, samples taken at different survey times assemble on different sides of axes. *DO* and *Chl* are positively correlated, but negatively correlated with *v* and M_2. These factors are distributed along the axes-two of RDA. Samples taken during the same survey time and from the same side of the confluence are relatively clustered. The Poyang Lake side had higher values of *DO* and *Chl*, while the Yangtze River side had faster flow and higher hydraulic complexity.

The first two axes explain a total of 44.38 % of the variance in fish community traits. They indicate the important contribution made by hydraulic and water quality factors to the relationship between fish communities and habitat factors at the confluence. Fish density was positively correlated with *v*, but negatively correlated with *Chl*, and was largely decided by the different habitat conditions between the Yangtze River and Poyang Lake, as a large part of fish abundance was observed in the Yangtze River with high velocity. The number of fish species and three biodiversity indexes were all positively correlated with *DO*, but negatively correlated with *Turb*. On the other hand, a negative correlation was observed between the relative abundance of *Z. platypus* and *Turb*, while the relative abundance of *H. molitrix*, *P. parva*, and *C. nasus* were positively influenced by *Turb*. The result shows that the high turbidity environment occurred in Survey 2 largely contributed to the change of species assemblage structure of the fish community near the confluence. Fish species in Group A were able to tolerate the large increase in turbidity, and their relative abundance increased from Survey 1 to Survey 2. However, most other fish species could not tolerate such environmental changes and were forced to relocated out of the confluence, which is an important reason why fish species number near the confluence substantially decreased between the two surveys. Previous literature studies had similar views about the effect of turbidity on fish. Robertis et al. (2003) conducted a series of laboratory feeding experiments and found that turbidity disproportionately decreased feeding efficiency of different fish; turbid environments benefited planktivorous fish since they were less vulnerable to predation by piscivores, while their feeding ability did not decrease substantially. Mol and Ouboter (2004) compared the fish communities in streams affected by gold

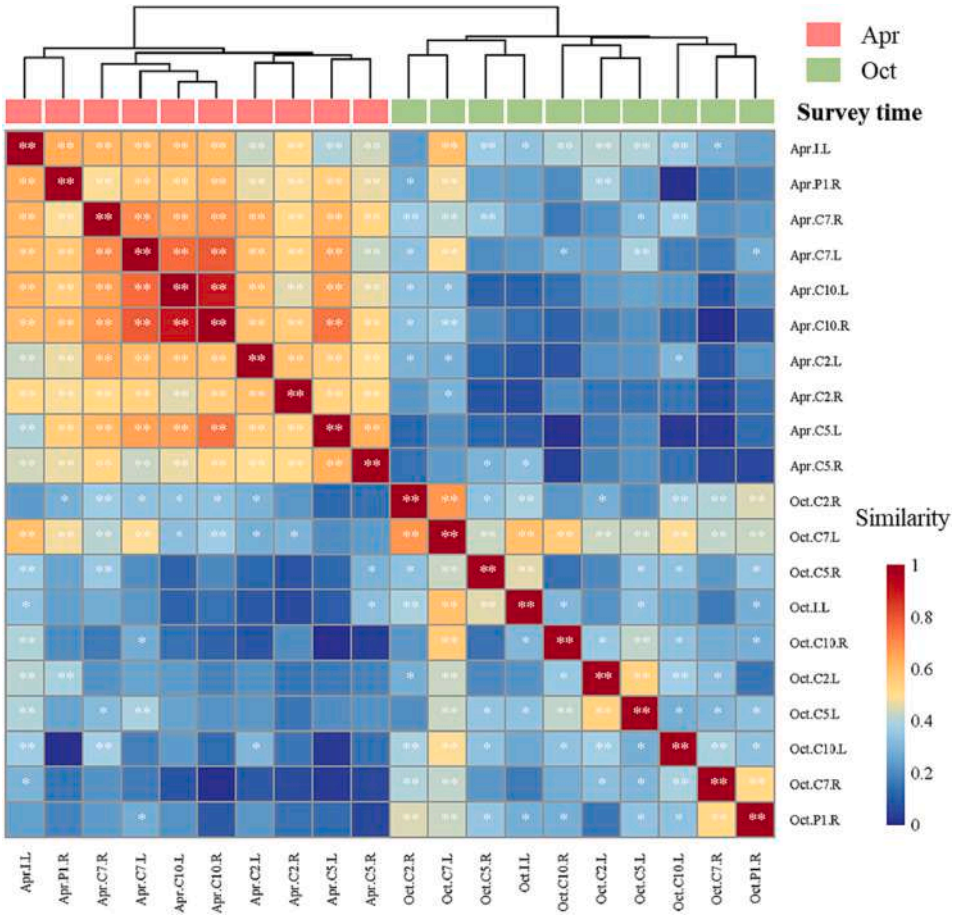

Fig. 13. Heatmap of similarities among different sampling sites based on fish species and relative abundance. The color of the block represents the magnitude of the correlation coefficient. The * in the block represents the significance of the correlation. The dendrogram shows the relationship of sites based on UPGMA clustering method.

mining with those in undisturbed streams in a South American tropical rainforest system and found that high turbidity related to the gold mining reduced fish diversity and thus shifted community structure.

The abundance distribution and species assemblage structure of fish communities, near the confluence between the Yangtze River and the Poyang Lake outflow channel, are driven by the spatiotemporal variation of different habitat factors (Table 4). At the regional scale, while the hydrodynamic conditions between the two surveys were similar, they had high spatial heterogeneity between the Yangtze River and the Poyang Lake outflow channel. The flow structure at the confluence greatly affected the spatial distribution of fish abundances. Specifically, small fish species or juvenile fish of some species prefer to be in YR and PC with high flow velocity rather than in PL. Although the proportion of small fish to total fish abundance in PL was higher in October, the absolute number of small fish was higher in YR and PC. The distribution of large-sized fish was less affected by the hydraulic factors, as they could choose their habitat more freely. Predator-prey interactions might explain this since small-sized fish that are more flexible need to take advantage of flow with high velocity and complex structure to escape from predators, even though this needs more effort to withstand the flow (Jones et al., 2020); large-sized fish free from predation pressure chose more suitable flow conditions to reduce energy consumption.

The sudden changes of water quality factors have a great impact on the diversity of fish species at the confluence. Between the two surveys, there was noticeable change in turbidity near the confluence, which greatly influenced the species assemblage structure of local fish communities. In April, local fish species diversity was high and good connectivity of the fish community across the confluence was observed. However, some fish species were not observed in October, possibly due to the onset of turbid environment near the confluence. Presumably, fish species observed in October tolerated the environmental conditions in which turbidity increased dramatically, while those not observed probably failed to tolerate and left the confluence. Consequently, the conditions in October led to a decline in the local species diversity with greater dominance of a few tolerated species. Such environmental constraints restrict different fish species to live in regions meeting their habitat demands, whereby the exchange of fish communities between tributaries is weakened.

3.5. *Nodal effect of confluence to river ecosystem and implication to ecological conservation and management*

During the two surveys, the merging flows from the Yangtze River and Poyang Lake had distinct physical and chemical properties and complex mixing processes were observed in the post-confluence channel, resulting in the heterogeneity and complexity of the spatial and temporal distribution of habitat conditions. Higher abundance and species diversity of fish community were observed in the post-confluence channel compared with both tributaries upstream, indicating the value of the river confluence as a biodiversity hotspot. Fernandes et al. (2004) investigated the fish communities in the Amazon River with trawl-net sampling, and found that the inflow of tributaries tended to increase the fish species diversity in the mainstream downstream of tributary confluences. Knispel and Castella (2003) investigated the benthic macroinvertebrate fauna in a glacier-fed stream at its confluence in Swiss Alps, and found the fauna was richer and more

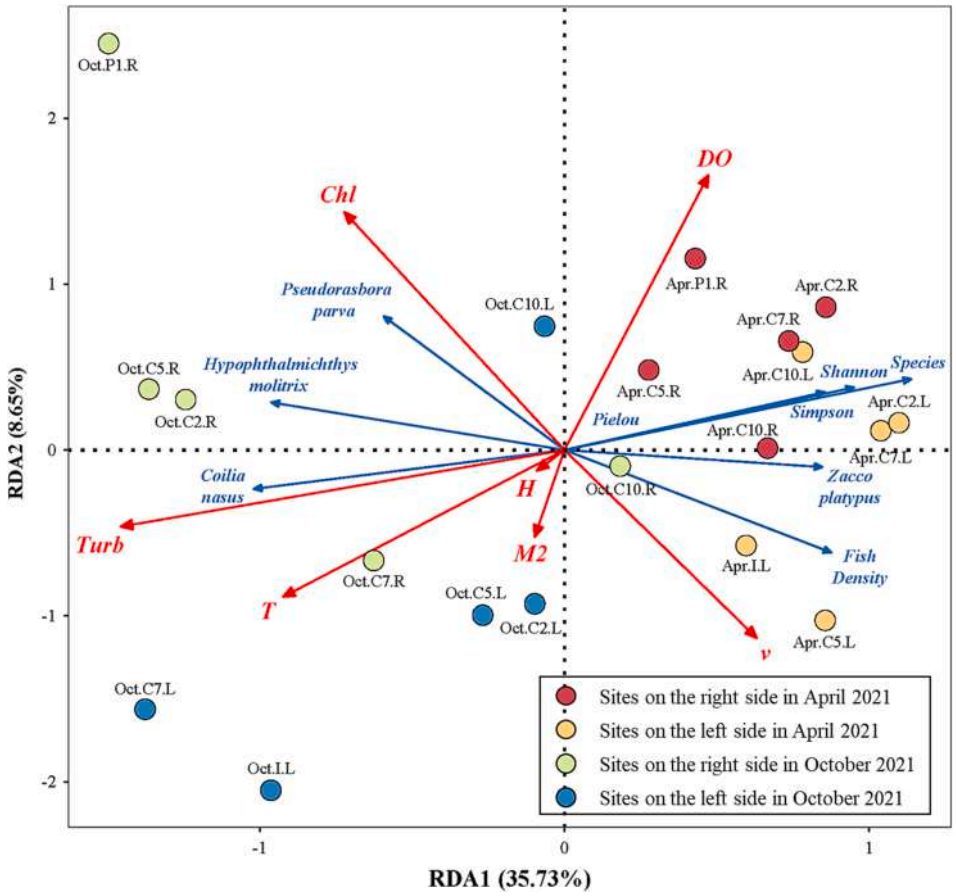

Fig. 14. Redundancy analysis (RDA) diagram for fish community traits and habitat factors of the confluence between the Yangtze River and the Poyang Lake outflow channel during Surveys 1 and 2. Habitat factors: water depth (*H*), velocity (*v*), hydraulic complexity metric M_2, temperature (*T*), dissolved oxygen concentration (*DO*), chlorophyll content (*Chl*), and turbidity (*Turb*).

diverse below the confluence. Osawa et al. (2010) measured riparian plant species diversity at 11 river confluences in Japan, and higher diversities were generally observed in down-confluence areas during the plant growing season. Therefore, it is of great significance for river ecological environment to recognize the important effect of confluences as critical nodes in river ecosystems. Specifically, further understanding of the effect of interaction between water and sediment, mixing dynamics, and habitat condition changes on biological communities at

Table 4
Summary of spatiotemporal distribution pattern of different habitat factors and their effect on fish communities at the confluence of the Yangtze River and the Poyang Lake outflow channel based on the two surveys in April and October.

Habitat factor		Comparison between different regions of the confluence	Comparison between different surveys	Effect on local fish community
Hydraulic factor	Water depth	Highest in PC; similar between PL and YR	Slight increase from Survey 1 to 2	No significant effect in present study
	Velocity	Higher in YR and PC than PL	Similar distribution pattern between Surveys 1 and 2	Greatly affects the abundance distribution; higher fish abundance was in YR with high flow velocity than that in PL; small fish tend to distribute in the fast-flowing tributary, while large fish were less affected by hydrodynamic conditions
	Hydraulic complexity metric M2	High in region with low kinetic energy, such as the stagnation zone and banks zone	Similar distribution pattern between Surveys 1 and 2	No significant effect in present study
Water quality factor	Turbidity	PL and YR respectively kept the highest or lowest values; with the proceeding of the mixing process between two tributaries, water quality conditions in	Drastic increase from Survey 1 to 2	Greatly affects the species assemblage structure; turbid environment lower local species diversity and weaken the interaction between fish communities
	Temperature	FPC were closer to that in YR than NPC	Increase in YR and PC; remain unchanged in PL from Survey 1 to 2	No significant effect in present study
	Dissolved oxygen concentration		Slight decrease from Survey 1 to 2	No significant effect in present study
	Chlorophyll content		Slight increase from Survey 1 to 2	No significant effect in present study

confluences, and paying more attention to confluence in river ecological conservation and management.

The abundance of small fish with a length of 2–3 cm in Poyang Lake channel was observed to increase substantially in the survey in October compared with that in April, and its proportion to the total fish population surged from 23.01 % in April to 69.59 % in October. Based on the length of the fish and the timing of their appearance, these newly emerged small fish are supposed to be mainly migratory juvenile fish that enter Poyang Lake from the Yangtze River for rearing, indicating that the confluence acts as an important nursery habitat during the migration of juvenile fish. The temporal variation of juvenile fish abundance at the confluence between the Yangtze River and Poyang Lake has also been observed by previous studies (Hu et al., 2011; Ren et al., 2022). Around the confluence, the peak abundance of sedentary juvenile fish such as *Hemiculter bleekeri* and *Siniperca chuatsi* occurs from May to June; the abundance of migratory juvenile fish, such as the four major Chinese carps and *Coilia nasus*, is relatively high from July to October and peaks in August (Liu et al., 2019). The crucial role of river confluences in recruitment success of freshwater fish highlights the demand to focus on the particular ecological needs of river confluence at key times, such as maintaining appropriate hydrological and hydrodynamic processes through measures such as hydraulic engineering regulation during critical periods of fish reproduction to ensure the smooth migration of fish.

In the survey in October, an intrusion of turbid flow from Poyang Lake to the Yangtze River was observed to significantly affect the species assemblage structure of fish communities around the confluence, which decreased the diversity of local fish species and weakened the exchange of fish communities between the river and the lake. The turbid flow was probably caused by sand mining events in the tributary, which often resulted in a high concentration of suspended sediment in the water. The high concentration of suspended sediment flows into the mainstream along with the tributary, leading to the disappearance of some sand-averse fish species at the confluence. The dramatic change of the physical and chemical properties in the tributary tends to be transmitted to the mainstream through the nodal effects of the confluence, affecting a wider community of organisms (Braaten et al., 1999; Rice et al., 2006; Baldigo et al., 2015). Therefore, it is necessary to strictly regulate anthropogenic activities such as sand mining and pollution discharge in tributaries of river confluences to prevent potential damage to river ecosystems.

CRediT authorship contribution statement

Saiyu Yuan: Investigation, Supervision, Methodology, Formal analysis, Writing – review & editing. **Jiajian Qiu:** Investigation, Methodology, Formal analysis, Visualization, Writing – original draft. **Hongwu Tang:** Supervision, Methodology, Funding acquisition, Resources, Writing – review & editing. **Lei Xu:** Investigation, Visualization. **Yang Xiao:** Supervision, Resources. **Mengyang Liu:** Writing – review & editing. **Colin Rennie:** Formal analysis, Writing – review & editing. **Carlo Gualtieri:** Validation, Visualization, Formal analysis, Writing – review & editing.

Declaration of Competing Interest

The authors declare that they have no known competing financial interests or personal relationships that could have appeared to influence the work reported in this paper.

Data availability

Data will be made available on request.

Acknowledgments

This research was funded by the National Key R&D Program of China (2022YFC3202602), the National Natural Science Foundation of China (U2040205; 52079044), the Fok Ying Tung Education Foundation (520013312), and the 111 Project (B17015). The authors would like to thank Professor Bidya Sagar Pani of the Indian Institute of Technology-Bombay for help in revising this work. Thanks are also extended to Xiao Luo, Yunqiang Zhu, Hao Wang, Supeng Wang, Guanghui Yan, Ping Wang and Jiaming Yang of Hohai University for their support during the field surveys.

References

Asaeda, T., Vu, T.K., Manatunge, J., 2005. Effects of flow velocity on feeding behavior and microhabitat selection of the stone Moroko Pseudorasbora parva: a trade-off between feeding and swimming costs. Trans. Am. Fish. Soc. 134, 537–547. https://doi.org/10.1577/T03-083.1.

Baldigo, B.P., George, S.D., Keller, W.T., 2015. Fish assemblages in the upper Esopus Creek, NY: current status, variability, and controlling factors. Northeast. Nat. 22, 345–371. https://doi.org/10.1656/045.022.0209.

Bean, C.W., Winfield, I.J., Fletcher, J.M., 1996. Stock assessment of the Arctic Charr (*Salvelinus alpinus*) population in Loch Ness, UK, Stock Assessment in Inland Fisheries. Fishing News Books, Blackwell, Scientific Publications, Oxford.

Beaugrand, G., Brander, K.M., Lindley, J.A., Souissi, S., Reid, P.C., 2003. Plankton effect on cod recruitment in the North Sea. Nature 426, 661–664. https://doi.org/10.1038/nature02164.

Bergman, J., Neigel, K., Landsman, S., Glassman, D., LaRochelle, L., Bennett, J., Rennie, C., Vermaire, J., Cooke, S., 2023. Multi-year evaluation of muskellunge (Esox masquinongy) spatial ecology during winter drawdowns in a regulated, urban waterway in Canada. Hydrobiologia 850, 417–439. https://doi.org/10.1007/s10750-022-05083-3.

Best, J.L., 1987. Flow dynamics at river channel confluences: implications for sediment transport and bed morphology. Recent Dev. Fluv. Sedimentol. 27–35 https://doi.org/10.2110/pec.87.39.0027.

Best, J.L., 1988. Sediment transport and bed morphology at river channel confluences. Sedimentology 35, 481–498. https://doi.org/10.1111/j.1365-3091.1988.tb00999.x.

Best, J.L., Roy, A., 1991. Mixing-layer distortion at the confluence of channels of different depth. Nature 350, 411–413. https://doi.org/10.1038/350411a0.

Boswell, K.M., David Wells, R.J., Cowan, J.H., Wilson, C.A., 2010. Biomass, density, and size distributions of fishes associated with a large-scale Artificial Reef complex in the Gulf of Mexico. Bull. Mar. Sci. 86, 879–889. https://doi.org/10.5343/bms.2010.1026.

Braaten, P.J., Guy, C.S., 1999. Relations between physicochemical factors and abundance of fishes in tributary confluences of the lower channelized Missouri river. Trans. Am. Fish. Soc. 128, 1213–1221. https://doi.org/10.1577/1548-8659(1999)128<1213:rbpfaa>2.0.co;2.

Brehmer, P., Chi, T.D., Mouillot, D., 2006. Amphidromous fish school migration revealed by combining fixed sonar monitoring (horizontal beaming) with fishing data. J. Exp. Mar. Bio. Ecol. 334, 139–150. https://doi.org/10.1016/j.jembe.2006.01.017.

Brown, J.H., Gillooly, J.F., Allen, A.P., Savage, V.M., West, G.B., 2004. Toward a metabolic theory of ecology. Ecology 85, 1771–1789. https://doi.org/10.1890/03-9000.

Campodonico, V.A., García, M.G., Pasquini, A.I., 2015. The dissolved chemical and isotopic signature downflow the confluence of two large rivers: the case of the Parana and Paraguay rivers. J. Hydrol. 528, 161–176. https://doi.org/10.1016/j.jhydrol.2015.06.027.

Cheng, D., Song, J., Wang, W., Zhang, G., 2019. Influences of riverbed morphology on patterns and magnitudes of hyporheic water exchange within a natural river confluence. J. Hydrol. 574, 75–84. https://doi.org/10.1016/j.jhydrol.2019.04.025.

Constantinescu, G., Miyawaki, S., Rhoads, B., Sukhodolov, A., Kirkil, G., 2011. Structure of turbulent flow at a river confluence with momentum and velocity ratios close to 1: Insight provided by an eddy-resolving numerical simulation. Water Resour. Res. 47 https://doi.org/10.1029/2010WR010018.

Constantinescu, G., Miyawaki, S., Rhoads, B., Sukhodolov, A., 2012. Numerical analysis of the effect of momentum ratio on the dynamics and sediment-entrainment capacity of coherent flow structures at a stream confluence. J. Geophys. Res. Surf. 117 (F4) https://doi.org/10.1029/2012JF002452.

Constantinescu, G., Miyawaki, S., Rhoads, B., Sukhodolov, A., 2016. Influence of planform geometry and momentum ratio on thermal mixing at a stream confluence with a concordant bed. Environ. Fluid Mech. 16, 845–873. https://doi.org/10.1007/s10652-016-9457-0.

Crowder, D.W., Diplas, P., 2000. Evaluating spatially explicit metrics of stream energy gradients using hydrodynamic model simulations. Can. J. Fish. Aquat. Sci. 57, 1497–1507. https://doi.org/10.1139/f00-074.

Crowder, D.W., Diplas, P., 2002. Vorticity and circulation: Spatial metrics for evaluating flow complexity in stream habitats. Can. J. Fish. Aquat. Sci. 59, 633–645. https://doi.org/10.1139/f02-037.

Dabiri, J.O., 2017. How fish feel the flow. Nature 547, 406–407. https://doi.org/10.1038/nature23096.

Duguay, J., Biron, P.M., Lacey, J., 2022. Impact of density gradients on the secondary flow structure of a river confluence. Water Resour. Philos. Phenomenol. Res. 58 https://doi.org/10.1029/2022WR032720.
Egerton, J.P., Bolser, D.G., Grüss, A., Erisman, B.E., 2021. Understanding patterns of fish backscatter, size and density around petroleum platforms of the U.S. Gulf of Mexico using hydroacoustic data. Fish. Res. 233, 105752 https://doi.org/10.1016/j.fishres.2020.105752.
Fan, Z., Ba, J., Duan, X., 2012. Studies on fish resources and species diversity in the middle reaches of the Yangtze River from Yichang to Chenglingji section. Freshw. Fish. 42, 20–25 https://doi.org/1000-6907(2012)42:4<20:CJYCDC>2.0.TX;2-G.
Fang, D., Yang, H., Zhang, H., Wu, J., Wei, Q., 2023. Fish community structure and diversity in the middle reaches of the Yangtze River. J. Fish. China 47, 029311. https://doi.org/10.11964/jfc.20220813657.
Fernandes, C.C., Podos, J., Lundberg, J.G., 2004. Amazonian ecology: tributaries enhance the diversity of electric fishes. Science (80-) 305, 1960–1962. https://doi.org/10.1126/science.1101240.
Gualtieri, C., Ianniruberto, M., Filizola, N., Santos, R., Endreny, T., 2017. Hydraulic complexity at a large river confluence in the Amazon basin. Ecohydrology 10, e1863. https://doi.org/10.1002/eco.1863.
Gualtieri, C., Filizola, N., Oliveira, M., Santos, A.M., Ianniruberto, M., 2018. A field study of the confluence between Negro and Solimões Rivers. Part 1: hydrodynamics and sediment transport. Comptes Rendus Geosci. 350, 31–42. https://doi.org/10.1016/j.crte.2017.09.015.
Gualtieri, C., Ianniruberto, M., Filizola, N., 2019. On the mixing of rivers with a difference in density: the case of the Negro/Solimões confluence, Brazil. J. Hydrol. 578, 124029 https://doi.org/10.1016/j.jhydrol.2019.124029.
Gualtieri, C., Abdi, R., Ianniruberto, M., Filizola, N., Endreny, T.A., 2020. A 3D analysis of spatial habitat metrics about the confluence of Negro and Solimões rivers, Brazil. Ecohydrology 13, e2166. https://doi.org/10.1002/eco.2166.
Hänfling, B., Handley, L.L., Read, D.S., Hahn, C., Li, J., Nichols, P., Blackman, R.C., Oliver, A., Winfield, I.J., 2016. Environmental DNA metabarcoding of lake fish communities reflects long-term data from established survey methods. Mol. Ecol. 25, 3101–3119. https://doi.org/10.1111/mec.13660.
Hu, Q., Feng, S., Guo, H., Chen, G., Jiang, T., 2007. Interactions of the Yangtze river flow and hydrologic processes of the Poyang Lake, China. J. Hydrol. 347, 90–100. https://doi.org/10.1016/j.jhydrol.2007.09.005.
Hu, M., Wu, Z., Liu, Y., 2011. Time course of the juvenile major Chinese carps in the Hukou waters of Poyang Lake. Resour. Environ. Yangtze Basin 20, 534–539 https://doi.org/1004-8227(2011)20:5<534:PYHHKS>2.0.TX;2-R.
Hui, C., Li, Y., Liao, Z., Zhang, W., Zhang, H., Niu, L., Wang, L., 2022. Confluences characteristics determine the influence scope of microbial community from confluence hydrodynamic zone on river network. J. Hydrol. 612, 128288 https://doi.org/10.1016/j.jhydrol.2022.128288.
Jo, T., Yamanaka, H., 2022. Meta-analyses of environmental DNA downstream transport and deposition in relation to hydrogeography in riverine environments. Freshw. Biol. 67, 1333–1343. https://doi.org/10.1111/fwb.13920.
Jones, P.E., Svendsen, J.C., Börger, L., Champneys, T., Consuegra, S., Jones, J.A.H., De Leaniz, C.G., 2020. One size does not fit all: Inter- and intraspecific variation in the swimming performance of contrasting freshwater fish. Conserv. Physiol. 8, coaa126. https://doi.org/10.1093/conphys/coaa126.
Knispel, S., Castella, E., 2003. Disruption of a longitudinal pattern in environmental factors and benthic fauna by a glacial tributary. Freshw. Biol. 48, 604–618. https://doi.org/10.1046/j.1365-2427.2003.01030.x.
Konsoer, K.M., Rhoads, B.L., 2014. Spatial–temporal structure of mixing interface turbulence at two large river confluences. Environ. Fluid Mech. 14, 1043–1070. https://doi.org/10.1007/s10652-013-9304-5.
Kramer, D.L., 1987. Dissolved oxygen and fish behavior. Environ. Biol. Fishes 18, 81–92. https://doi.org/10.1007/BF00002597.
Lacey, R.W., Neary, V.S., Liao, J.C., Enders, E.C., Tritico, H.M., 2012. The IPOS framework: Linking fish swimming performance in altered flows from laboratory experiments to rivers. River Res. Appl. 28, 429–443. https://doi.org/10.1002/rra.1584.
Li, K., Tang, H., Yuan, S., Xiao, Y., Xu, L., Huang, S., Rennie, C.D., Gualtieri, C., 2022. A field study of near-junction-apex flow at a large river confluence and its response to the effects of floodplain flow. J. Hydrol. 610, 127983 https://doi.org/10.1016/j.jhydrol.2022.127983.
Lin, P.C., Gao, X., Liu, F., Li, M.Z., Liu, H.Z., 2021. Ecological assessment of the yangtze river environment based on fish species richness. Acta Hydrobiol. Sin. 45, 1385–1389. https://doi.org/10.7541/2021.2021.0269.
Liu, S., Duan, X., Chen, D., Liao, F., Chen, W., 2005. Studies on status of fishery resources in the middle reach of the Yangtze River. Acta Hydrobiol. Sin. 29, 708–711 https://doi.org/1000-3207(2005)29:6<708:CJZYYY>2.0.TX;2-#.
Liu, Y., Yang, X., Ren, P., Li, X., Fang, D., Xu, D., 2019. Community characteristics of larvae and juvenile fish in Hukou section of the Yangtze River in spring and summer. Acta Hydrobiol. Sin. 43, 142–154. https://doi.org/10.7541/2019.018.
Love, R., 1971. Measurements of fish target strength: a review. Fish. Bull. 69, 703–715.
Luis, S.M., Pasternack, G.B., 2023. Local hydraulics influence habitat selection and swimming behavior in adult California Central Valley Chinook salmon at a large river confluence. Fish. Res. 261, 106634 https://doi.org/10.1016/j.fishres.2023.106634.
Mol, J.H., Ouboter, P.E., 2004. Downstream effects of erosion from small-scale gold mining on the instream habitat and fish community of a small neotropical rainforest stream. Conserv. Biol. 18, 201–214. https://doi.org/10.1111/j.1523-1739.2004.00080.x.
Moses, A.P., Staton, B.A., Smith, N.J., 2019. Migratory timing and rates of Chinook salmon bound for the Kwethluk and Kisaralik rivers. J. Fish Wildl. Manag. 10, 419–431. https://doi.org/10.3996/082018-JFWM-074.
Northcote, T., 1996. Migratory behaviour of fish and its significance to movement through riverine fish passage facilities. In: Jungwirth, M., Schmutz, S., Weiss, S. (Eds.), Symposium on Fish Migration and Fish Bypasses. Vienna, Austria, pp. 3–18.
Olivetti, S., Gil, M.A., Sridharan, V.K., Hein, A.M., 2021. Merging computational fluid dynamics and machine learning to reveal animal migration strategies. Methods Ecol. Evol. 12, 1186–1200. https://doi.org/10.1111/2041-210X.13604.
Osawa, T., Mitsuhashi, H., Ushimaru, A., 2010. River confluences enhance riparian plant species diversity. Plant Ecol. 209, 95–108. https://doi.org/10.1007/s11258-010-9726-9.
Pickering, C., Ford, W.I., 2021. Effect of watershed disturbance and river-tributary confluences on watershed sedimentation dynamics in the Western Allegheny Plateau. J. Hydrol. 602, 126784 https://doi.org/10.1016/j.jhydrol.2021.126784.
Port, J.A., O'Donnell, J.L., Romero-Maraccini, O.C., Leary, P.R., Litvin, S.Y., Nickols, K.J., Yamahara, K.M., Kelly, R.P., 2016. Assessing vertebrate biodiversity in a kelp forest ecosystem using environmental DNA. Mol. Ecol. 25, 527–541. https://doi.org/10.1111/mec.13481.
Ren, P., Hou, G., Schmidt, B.V., Fang, D., Xu, D., 2022. Longitudinal drifting pattern of larval assemblages in the lower reach of the Yangtze River: Impact of the floodplain lakes and conservation implementation. Ecol. Freshw. Fish 31, 410–423. https://doi.org/10.1111/eff.12640.
Rhoads, B.L., Johnson, K.K., 2018. Three-dimensional flow structure, morphodynamics, suspended sediment, and thermal mixing at an asymmetrical river confluence of a straight tributary and curving main channel. Geomorphology 323, 51–69. https://doi.org/10.1016/j.geomorph.2018.09.009.
Rhoads, B.L., Sukhodolov, A.N., 2008. Lateral momentum flux and the spatial evolution of flow within a confluence mixing interface. Water Resour. Res. 44 https://doi.org/10.1029/2007WR006634.
Rhoads, B.L., Riley, J.D., Mayer, D.R., 2009. Response of bed morphology and bed material texture to hydrological conditions at an asymmetrical stream confluence. Geomorphology 109, 161–173. https://doi.org/10.1016/j.geomorph.2009.02.029.
Rice, S.P., Ferguson, R.I., Hoey, T.B., 2006. Tributary control of physical heterogeneity and biological diversity at river confluences. Can. J. Fish. Aquat. Sci. 63, 2553–2566. https://doi.org/10.1139/F06-145.
Riley, J.D., Rhoads, B.L., 2012. Flow structure and channel morphology at a natural confluent meander bend. Geomorphology 163, 84–98. https://doi.org/10.1016/j.geomorph.2011.06.011.
Robertis, A., Ryer, C.H., Veloza, A., Brodeur, R.D., 2003. Differential effects of turbidity on prey consumption of piscivorous and planktivorous fish. Can. J. Fish. Aquat. Sci. 60, 1517–1526. https://doi.org/10.1139/f03-123.
Röpke, C.P., Amadio, S.A., Winemiller, K.O., Zuanon, J., 2016. Seasonal dynamics of the fish assemblage in a floodplain lake at the confluence of the Negro and Amazon Rivers. J. Fish Biol. 89, 194–212. https://doi.org/10.1111/jfb.12791.
Scarabotti, P.A., López, J.A., Pouilly, M., 2011. Flood pulse and the dynamics of fish assemblage structure from neotropical floodplain lakes. Ecol. Freshw. Fish 20, 605–618. https://doi.org/10.1111/j.1600-0633.2011.00510.x.
Shen, X., Li, R., Hodges, B.R., Feng, J., Cai, H., Ma, X., 2019. Experiment and simulation of supersaturated total dissolved gas dissipation: Focus on the effect of confluence types. Water Res. 155, 320–332. https://doi.org/10.1016/j.watres.2019.02.056.
Shen, X., Hodges, B.R., Li, R., Li, Z., Fan, J.L., Cui, N.B., Cai, H.J., 2021. Factors influencing distribution characteristics of total dissolved gas supersaturation at confluences. Water Resour. Res. 57 https://doi.org/10.1029/2020WR028760.
Shen, X., Li, R., Cai, H., Feng, J., Wan, H., 2022. Characteristics of secondary flow and separation zone with different junction angle and flow ratio at river confluences. J. Hydrol. 614, 128537 https://doi.org/10.1016/j.jhydrol.2022.128537.
Silva, A.T., Katopodis, C., Santos, J.M., Ferreira, M.T., Pinheiro, A.N., 2012. Cyprinid swimming behaviour in response to turbulent flow. Ecol. Eng. 44, 314–328. https://doi.org/10.1016/j.ecoleng.2012.04.015.
Smith, C.L., Powell, C.R., 1971. The summer fish communities of Brier Creek, Marshall County, Oklahoma. Am. Museum Novit. 2458, 1–30. https://doi.org/10.3828/bhs.48.1.1.
Song, Y., Cheng, F., Murphy, B.R., Xie, S., 2018. Downstream effects of the Three Gorges Dam on larval dispersal, spatial distribution, and growth of the four major Chinese carps call for reprioritizing conservation measures. Can. J. Fish. Aquat. Sci. 75, 141–151. https://doi.org/10.1139/cjfas-2016-0278.
Sukhodolov, A.N., Krick, J., Sukhodolova, T.A., Cheng, Z., Rhoads, B.L., Constantinescu, G.S., 2017. Turbulent flow structure at a discordant river confluence: asymmetric jet dynamics with implications for channel morphology. J. Geophys. Res. Earth Surf. 122, 1278–1293. https://doi.org/10.1002/2016JF004126.
Sutherland, A.B., Meyer, J.L., 2007. Effects of increased suspended sediment on growth rate and gill condition of two southern Appalachian minnows. Environ. Biol. Fishes 80, 389–403. https://doi.org/10.1007/s10641-006-9139-8.
Tang, H., Zhang, H., Yuan, S., 2018. Hydrodynamics and contaminant transport on a degraded bed at a 90-degree channel confluence. Environ. Fluid Mech. 18, 443–463. https://doi.org/10.1007/s10652-017-9562-8.
Vanni, M.J., Layne, C.D., 1997. Nutrient recycling and herbivory as mechanisms in the "'top-down'" effect of fish on algae in lakes. Ecology 78, 21–40. https://doi.org/10.1890/0012-9658(1997)078[0021:NRAHAM]2.0.CO;2.

Wenger, S.J., Isaak, D.J., Luce, C.H., Neville, H.M., Fausch, K.D., Dunham, J.B., Dauwalter, D.C., Young, M.K., Elsner, M.M., Rieman, B.E., Hamlet, A.F., Williams, J. E., 2011. Flow regime, temperature, and biotic interactions drive differential declines of trout species under climate change. PNAS 108, 14175–14180. https://doi.org/10.1073/pnas.1103097108.

Xie, R., Zhao, G., Yang, J., Wang, Z., Xu, Y., Zhang, X., Wang, Z., 2021. eDNA metabarcoding revealed differential structures of aquatic communities in a dynamic freshwater ecosystem shaped by habitat heterogeneity. Environ. Res. 201, 111602 https://doi.org/10.1016/j.envres.2021.111602.

Xu, Z., Yin, X., Sun, T., Cai, Y., Ding, Y., Yang, W., Yang, Z., 2017. Labyrinths in large reservoirs: An invisible barrier to fish migration. Water Resour. Res. 53, 817–831. https://doi.org/10.1002/2016WR019485.

Xu, L., Yuan, S., Tang, H., Qiu, J., Xiao, Y., Whittaker., C., Gualtieri, C., 2022. Mixing dynamics at the large confluence between the Yangtze River and Poyang Lake. Water Resour. Res. 58, e2022WR032195 https://doi.org/10.1029/2022WR032195.

Yang, M., Sheng, P., Zhang, Y., Guo, L., Wang, H., Gao, X., Chen, Y., 2022. Characteristics of fish assemblages of Poyang lake at the initial stage of the fishing ban. Acta Hydrobiol. Sin. 46, 1569–1579. https://doi.org/10.7541/2023.2022.0161.

Yuan, S., Tang, H., Xiao, Y., Qiu, X., Zhang, H., 2016. Turbulent flow structure at a 90-degree open channel confluence: accounting for the distortion of the shear layer. J. Hydro-Environ. Res. 12, 130–147. https://doi.org/10.1016/j.jher.2016.05.006.

Yuan, S., Tang, H., Xiao, Y., Qiu, X., Xia, Y., 2018. Water flow and sediment transport at open-channel confluences: an experimental study. J. Hydraul. Res. 56, 333–350. https://doi.org/10.1080/00221686.2017.1354932.

Yuan, S., Tang, H., Xiao, Y., Xia, Y., Melching, C., Li, Z., 2019. Phosphorus contamination of the surface sediment at a river confluence. J. Hydrol. 573, 568–580. https://doi.org/10.1016/j.jhydrol.2019.02.036.

Yuan, S., Tang, H., Li, K., Xu, L., Xiao, Y., Gualtieri, C., Rennie, C., Melville, B., 2021. Hydrodynamics, sediment transport and morphological features at the confluence between the Yangtze river and the Poyang Lake. Water Resour. Philos. Phenomenol. Res. 57 https://doi.org/10.1029/2020WR028284.

Yuan, S., Xu, L., Tang, H., Xiao, Y., Whittaker, C., 2022a. Swimming behavior of juvenile silver carp near the separation zone of a channel confluence. Int. J. Sedim. Res. 37, 122–127. https://doi.org/10.1016/j.ijsrc.2021.08.002.

Yuan, S., Xu, L., Tang, H., Xiao, Y., Gualtieri, C., 2022b. The dynamics of river confluences and their effects on the ecology of aquatic environment: a review. J. Hydrodyn. 34, 1–14. https://doi.org/10.1007/s42241-022-0001-z.

Zhang, T., Feng, M., Chen, K., Cai, Y., 2020. Spatiotemporal distributions and mixing dynamics of characteristic contaminants at a large asymmetric confluence in northern China. J. Hydrol. 591, 125583 https://doi.org/10.1016/j.jhydrol.2020.125583.